Development 125, 1123-1136 (1998)
Printed in Great Britain © The Company of Biologists Limited 1998
DEV2251

Hoxa1 and *Hoxb1* synergize in patterning the hindbrain, cranial nerves and second pharyngeal arch

Anthony Gavalas[1,*], Michèle Studer[2,†,*], Andrew Lumsden[3], Filippo M. Rijli[1,‡], Robb Krumlauf[2] and Pierre Chambon[1,‡]

[1]Institut de Génétique et de Biologie Moléculaire and Cellulaire, CNRS/INSERM/ULP, Collège de France, BP 163 - 67404 Illkirch Cedex, CU de Strasbourg, France
[2]Division of Developmental Neurobiology, MRC National Institute for Medical Research, The Ridgeway, Mill Hill, London NW7 1AA, UK
[3]Department of Developmental Neurobiology, UMDS, Guy's Hospital, London SE1 9RT, UK
*These authors contributed equally to this work
†Present address: Department of Developmental Neurobiology, UMDS, Guy's Hospital, London SE1 9RT, UK
‡Corresponding authors (E-mail: igbmc@igbmc.u-strasbg.fr; rijli@igbmc.u-strasbg.fr)

Accepted 22 December 1997: published on WWW 17 February 1998

SUMMARY

The analysis of *Hoxa1* and *Hoxb1* null mutants suggested that these genes are involved in distinct aspects of hindbrain segmentation and specification. Here we investigate the possible functional synergy of the two genes. The generation of *Hoxa1*$^{3'RARE}$/*Hoxb1*$^{3'RARE}$ compound mutants resulted in mild facial motor nerve defects reminiscent of those present in the *Hoxb1* null mutants. Strong genetic interactions between *Hoxa1* and *Hoxb1* were uncovered by introducing the *Hoxb1*$^{3'RARE}$ and *Hoxb1* null mutations into the *Hoxa1* null genetic background. *Hoxa1*^{null}/*Hoxb1*$^{3'RARE}$ and *Hoxa1*^{null}/*Hoxb1*^{null} double homozygous embryos showed additional patterning defects in the r4-r6 region but maintained a molecularly distinct r4-like territory. Neurofilament staining and retrograde labelling of motor neurons indicated that *Hoxa1* and *Hoxb1* synergise in patterning the VIIth through XIth cranial nerves. The second arch expression of neural crest cell markers was abolished or dramatically reduced, suggesting a defect in this cell population. Strikingly, the second arch of the double mutant embryos involuted by 10.5 dpc and this resulted in loss of all second arch-derived elements and complete disruption of external and middle ear development. Additional defects, most notably the lack of tympanic ring, were found in first arch-derived elements, suggesting that interactions between first and second arch take place during development. Taken together, our results unveil an extensive functional synergy between *Hoxa1* and *Hoxb1* that was not anticipated from the phenotypes of the simple null mutants.

Key words: Hindbrain, Patterning, Segmentation, RAREs, Cranial nerves, Neural crest, Ear development

INTRODUCTION

Extensive mutational analysis in the mouse has demonstrated the role of *Hox* genes in patterning the body of the developing embryo along the antero-posterior axis of the body and the proximo-distal axis of the limb (for reviews see Favier and Dollé, 1997; Rijli and Chambon, 1997). The anteriormost boundaries of vertebrate *Hox* gene expression lie in the hindbrain, the patterning of which proceeds through a segmentation process that is highly conserved in vertebrate evolution (Keynes and Lumsden, 1990; Keynes and Krumlauf, 1994; Wilkinson, 1995). This region of the neural tube is transiently divided, along the anteroposterior axis, into a series of 7-8 lineage-restricted compartments, the rhombomeres (r) (Fraser et al., 1990; Wingate and Lumsden, 1996; Lumsden and Krumlauf, 1996).

Loss-of-function mutants have been generated to analyse the genetic control of hindbrain segmentation and specification. Functional inactivation of the *Hoxa1* gene results in a complete (Chisaka et al., 1992; Carpenter et al., 1993) or near-complete deletion of rhombomere 5 (r5) (Lufkin et al., 1991; Mark et al., 1993; Dollé et al., 1993) and a severe reduction of r4, thus suggesting that Hoxa1 is acting in maintenance and/or generation of hindbrain segments, rather than in conferring a specific fate to them (Lufkin et al., 1991; Chisaka et al., 1992; Mark et al., 1993; Carpenter et al., 1993; Dollé et al., 1993). In contrast, Hoxb1 appears to be involved in conferring specific identity to r4 cells (Studer et al., 1996). Interestingly, in *Hoxa2* null mutants both segmentation and specification are affected, since the r1/r2 boundary is lost and r2 appears to be partially transformed into r1 (Gavalas et al., 1997). Krox20, a zinc finger transcription factor (Chavrier et al., 1988), is required for the maintenance of the r3 and r5 territories (Schneider-Maunoury et al., 1993, 1997; Swiatek and Gridley, 1993). Accordingly, Krox20 has been shown to be a direct or indirect regulator of *Hoxa2, Hoxb2, follistatin, Hoxb3* and *Sek1* in r3 and/or r5

(Sham et al., 1993; Nonchev et al., 1996; Vesque et al., 1996; Seitanidou et al., 1997). Kreisler (*kr*), a bZIP transcription factor (Cordes and Barsh, 1994), is necessary for establishment of r5 and r6 territories (Frohman et al., 1993; McKay et al., 1994) and appears to be a direct regulator of *Hoxb3* in r5 (Manzanares et al., 1997).

The hindbrain metameric organisation is reflected in the organisation of the associated cranial nerves. The trigeminal (Vth) nerve collects axons from motor nuclei lying in rhombomeres r1, r2 and r3, exits the brain from r2, and innervates the first branchial arch. The facioacoustic (VIIth/VIIIth) and glossopharyngeal (IXth) nerves collect axons from motor nuclei lying in r4/r5 and r6/r7, respectively, exit the brain from r4 (VIIth/VIIIth) and r6 (IXth) and innervate the second and the third branchial arches, respectively (Lumsden and Keynes, 1989; Marshall et al., 1992; Carpenter et al., 1993). The role of *Hox* genes in establishing the segmented, stereotyped pattern of motor neuron axonal projections and the organisation of cranial nerves has been investigated indirectly in mouse (Marshall et al., 1992; Kessel, 1993) and chick embryos (Gale et al., 1996; Nittenberg et al., 1997) by retinoic acid (RA) treatment, which induces ectopic *Hox* gene expression. Furthermore, the analysis of *Hox* loss-of-function mutants has shown that these genes influence the patterning of cranial nerves (Carpenter et al., 1993; Mark et al., 1993; Goddard et al., 1996; Studer et al., 1996; Barrow et al., 1996; Gavalas et al., 1997).

Rhombomere-specific generation of neural crest (NC) cells is observed along the dorsal part of the hindbrain, resulting in a segmental pathway of migration (Lumsden et al., 1991; Sechrist et al., 1993). The even-numbered rhombomeres and r1 generate the vast majority of hindbrain crest cells, whereas r3 and r5 are massively depleted from NC cells through apoptosis (Graham et al., 1993, 1994), generating small subpopulations that migrate rostrally and caudally into the arches (Sechrist et al., 1993; Köntges and Lumsden, 1996). Hindbrain NC cells migrate ventrally, giving rise to cranial sensory ganglia and populating the pharyngeal arches, thus contributing to the formation of muscular, skeletal and vascular structures (Le Lievre and Le Douarin, 1975; Noden, 1983; Couly et al., 1993; Köntges and Lumsden, 1996). A late-migrating subset of NC cells, which are derived exclusively from even-numbered rhombomeres and populate the prospective exit points of the cranial nerves, may provide chemoattractive signal(s) for outgrowing axons (Niederlander and Lumsden, 1996). Transplantation experiments suggest that the pharyngeal arch NC is responsible for specifying the fate of mesoderm (Noden, 1988; Trainor et al., 1995) and determining the muscle attachment points to the skeleton of the head (Köntges and Lumsden, 1996).

Hox genes play a major role in patterning the mesenchyme of the pharyngeal arches. The targeted inactivation of *Hoxa2* results in a homeotic transformation of the second arch neural crest-derived skeletal elements into first arch derivatives (Gendron-Maguire et al., 1993; Rijli et al., 1993), revealing the existence of a skeletogenic ground patterning program common to the NC of the second and part of the first arches (Rijli et al., 1993). *Hoxa3* null mutants show specific deletions or hypoplasias of structures derived from the third pharyngeal arch (Chisaka and Capecchi, 1991; Manley and Capecchi, 1995).

In view of the importance of *Hox* genes in all aspects of hindbrain development, it becomes important to understand the regulatory mechanisms establishing and maintaining their expression as well as the degree of their functional redundancy. In the accompanying paper (Studer et al., 1998) we show that, similarly to *Hoxa1* (Dupé et al., 1997, and references therein), a retinoic acid response element (RARE) is necessary for timely establishment of the early expression domain of *Hoxb1*. In turn, *Hoxa1* and *Hoxb1* are essential for establishing *Hoxb1* expression in the presumptive r4 through activation of a *Hoxb1* autoregulatory loop (Pöpperl et al., 1995). Simultaneous lack of *Hoxa1* and *Hoxb1* expression in the presumptive hindbrain leads to early patterning defects, not seen in any of the simple *Hoxa1* and *Hoxb1* null mutants (Studer et al., 1998). In this report, we investigate the late phenotypic alterations of double mutants lacking both *Hoxa1* and *Hoxb1* expression. In addition, we study the morphological consequences of impairing the early activation of both *Hoxa1* and *Hoxb1* by generating $Hoxa1^{3'RARE}/Hoxb1^{3'RARE}$ double homozygous mutants. Our findings show that *Hoxa1* and *Hoxb1* synergize in patterning the hindbrain, cranial nerves and derivatives of the pharyngeal arches.

MATERIALS AND METHODS

Whole-mount in situ hybridisation and immunostaining

Whole-mount in situ hybridisation was performed as described (Dupé et al., 1997), with the following modifications. Proteinase K treatment was for 5.5 minutes for 8.5 dpc embryos, 10 minutes for 9.5 dpc embryos and 15 minutes for 10.5 dpc embryos, and embryos were immediately fixed. The reaction for the colour development was done in 10% polyvinyl alcohol (31,000-50,000 kDa), 150 mM NaCl, 100 mM Tris, pH 9.5, and 25 mM $MgCl_2$.

Whole-mount immunostaining using the anti-neurofilament monoclonal antibody 2H3 (Developmental Studies Hybridoma Bank), the anti-Krox20 polyclonal antibody (Berkeley Antibody Company PRB-231P-100) and genotyping were done as described (Mark et al., 1993; Studer et al., 1998).

Retrograde labelling

Embryos were fixed in 4% paraformaldehyde in phosphate-buffered saline (PBS) and injected with the carbocyanine tracers DiI and DiO (Molecular Probes) in dimethyl-formamide (6 mg/ml). Injections, flat-mount preparations and analysis of retrogradely labeled specimens under a confocal microscope fitted with a 10× lens, were as described (Marshall et al., 1992), using fluorescein and rhodamine filters to visualise the DiO and DiI labelling, respectively. Two overlapping series of images, taken for wild-type (wt) specimens, were subsequently superimposed using Photoshop. A single series of images was taken for all mutants presented.

Scanning electron microscopy

Embryos were dissected in cold PBS, fixed overnight at 4°C in 2.5% glutaraldehyde in 0.1 M cacodylate buffer (pH 7.2), washed in cacodylate buffer for 30 minutes, dehydrated through a graded series of ethanol (50%, 70%, 90%, 100% in ddH_2O) for 30 minutes in each solution, and dried with a critical-point drying apparatus. Embryos were mounted on aluminum stubs and coated with palladium-gold using a cold sputter-coater, before photographing with a Philips Electron XL20 scanning electron microscope.

Histological and skeletal analysis

Mouse fetuses were fixed in Bouin's solution, dehydrated, cleared and embedded in parafin. Serial histological sections, 10 μm thick, were

stained with Groat's hematoxylin and Mallory's trichrome (Mark et al., 1993). For whole-mount analysis of skeletons and inner ears, fetuses were processed as described (Lufkin et al., 1991).

RESULTS

Lowering the response of both *Hoxa1* and *Hoxb1* to endogenous retinoids results in malformations of the facial nerve

Homozygous *Hoxa1*$^{3'RARE}$ embryos exhibited an initial delay in *Hoxa1* activation and subsequent mild segmentation and cranial nerve defects with a low penetrance. However, these defects were eventually compensated for, and homozygotes, born in the expected Mendelian ratio, were viable and fertile (Dupé et al., 1997). In homozygous *Hoxb1*$^{3'RARE}$ embryos there was a specific down-regulation of early *Hoxb1* neuroectodermal expression (Studer et al., 1998). Homozygotes were born in the expected Mendelian ratio and exhibited a low (5%) perinatal lethality (Fig. 1A). Dead newborns had no milk in their stomach, which indicated a feeding disability. A small fraction (5%) of the surviving homozygotes died at weaning (3rd-4th week) due to excessive growth of the incisor teeth, which block the oral cavity and prevent feeding (Fig. 1B). These mice survived when put on a semi-dry diet and had their teeth clipped regularly. The remainder of the *Hoxb1*$^{3'RARE}$ homozygotes were viable and fertile.

As *Hoxa1* appears to be necessary for the early establishment of *Hoxb1* expression (Studer et al., 1998), we asked whether impairing the early activation of both *Hoxa1* and *Hoxb1* would exacerbate the *Hoxb1*$^{3'RARE}$ defects. Indeed, the low penetrance of these defects was increased significantly as the two copies of the *Hoxa1* 3′ RARE were mutated (Fig. 1A). Given that similar defects were seen in the *Hoxb1*^{null} homozygotes (Goddard et al., 1996) and that the facial motor nerve of these mutants failed to develop normally (Goddard et al., 1996; Studer et al., 1996), the facial region of affected and unaffected animals was dissected and examined for the presence of the major facial motor nerve branches (Goddard et al., 1996; Fig. 1C). The hyomandibular branch was specifically missing in the affected animals, either unilaterally (in four *Hoxa1*$^{3'RARE}$/*Hoxb1*$^{3'RARE}$ double homozygous and two *Hoxa1*$^{3'RARE+/-}$/*Hoxb1*$^{3'RARE-/-}$ compound mutants) or bilaterally (in two *Hoxa1*$^{3'RARE}$/*Hoxb1*$^{3'RARE}$ double homozygous and one *Hoxa1*$^{3'RARE+/-}$/*Hoxb1*$^{3'RARE-/-}$ compound mutants) (Fig. 1D). The inability of newborns to feed could also reflect facial nerve defects, as this nerve innervates the muscles responsible for suckling. However, in contrast to the *Hoxb1*^{null} homozygotes (Goddard et al., 1996), affected animals did not show signs of facial paralysis but defects in the facial muscles have not been ruled out. Subsequent inbreeding of the surviving double homozygotes produced offspring in which the frequency of the perinatal lethality and the excessively long incisor teeth was reduced. This may reflect the mixed genetic background of the colony and the selection of animals with a genetic makeup compensating for the effect of the RARE mutations.

Skeletal analysis of simple and double mutant newborns, including affected animals, did not reveal any skeletal abnormalities. Hindbrain segmentation of *Hoxb1*$^{3'RARE}$ homozygous and *Hoxa1*$^{3'RARE}$/*Hoxb1*$^{3'RARE}$ double homozygous embryos was normal, with the exception, in the latter, of a low penetrance and stage-dependent slight reduction of rhombomere 5 (data not shown), which was also observed in the *Hoxa1*$^{3'RARE}$ homozygous mutants (Dupé et al., 1997).

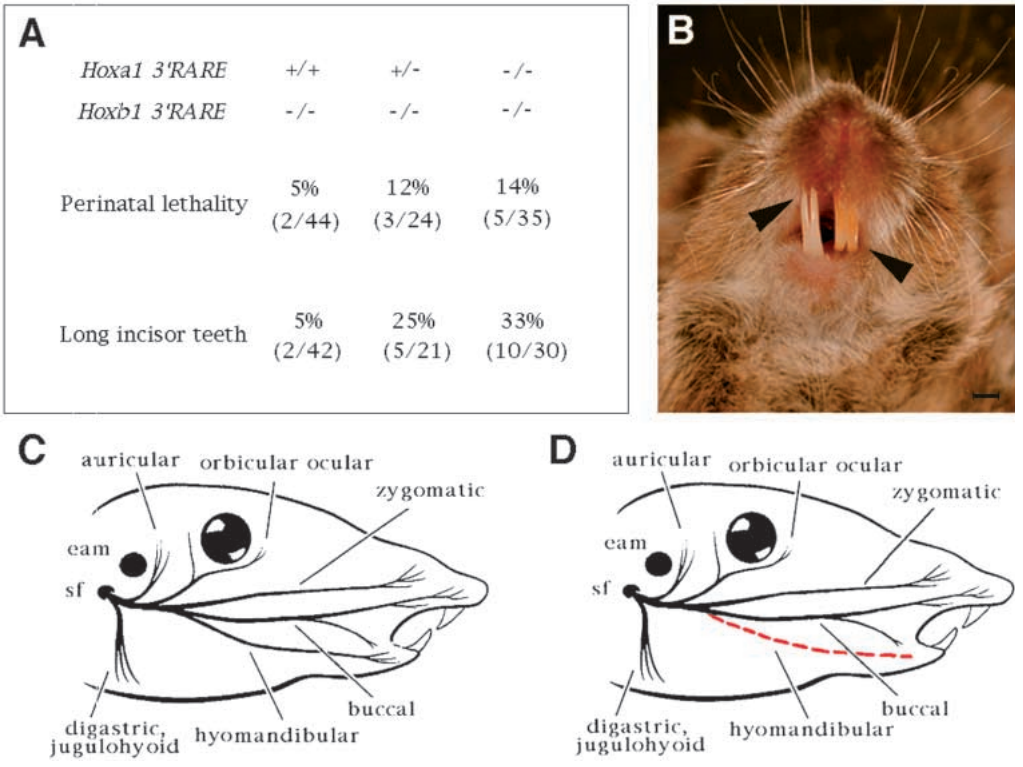

Fig. 1. Lethality and facial motor nerve malformations in *Hoxa1*$^{3'RARE}$/*Hoxb1*$^{3'RARE}$ compound mutants. (A) Frequencies of the perinatal (up to 1 day after birth) lethality and long incisor teeth (arrows in B), in the compound mutants generated. (C,D) Diagrams of the facial motor nerve of wild type and affected animals, respectively (adapted from Goddard et al., 1996). eam, external auditory meatus; sf, stylomastoid foramen. Scale bar, 1 mm.

Cranial nerve development of *Hoxb1*$^{3'RARE}$ homozygous and *Hoxa1*$^{3'RARE}$/*Hoxb1*$^{3'RARE}$ double homozygous embryos was examined at 10.5 dpc by whole-mount immunostaining and retrograde labelling of the trigeminal (V) and facial (VII) motor neurons. No defects were found with the exception, in the *Hoxa1*$^{3'RARE}$/*Hoxb1*$^{3'RARE}$ double homozygous embryos, of a low penetrance unilateral loss of the proximal part of the glossopharyngeal (IX) nerve (data not shown), which was also found in the *Hoxa1*$^{3'RARE}$ homozygous mutants (Dupé et al., 1997).

In summary, despite significant down-regulation of r4 *Hoxb1* expression in one third of the *Hoxa1*$^{3'RARE}$/*Hoxb1*$^{3'RARE}$ double homozygous embryos examined (Studer et al., 1998), only mild defects in the facial motor nerve were subsequently detected in these mutants (Table 1).

Defects in the hindbrain of *Hoxa1*^{null}/*Hoxb1*$^{3'RARE}$ and *Hoxa1*^{null}/*Hoxb1*^{null} double homozygous embryos

The combined lack of *Hoxa1* and *Hoxb1* expression resulted in early loss of the r4 expression of *EphA2* (Studer et al., 1998), which was not observed in either *Hoxa1* or *Hoxb1* simple null mutants. This finding indicated that *Hoxa1* and *Hoxb1* synergise in early patterning of this territory and raised the possibility that these genes have partially redundant functions in establishing r4 identity.

Krox20 was used as a marker for r3 and r5 territories (Wilkinson et al., 1989a) to examine the hindbrain segmentation of *Hoxa1*^{null}/*Hoxb1*$^{3'RARE}$ double homozygous embryos, in which *Hoxb1* expression is specifically abolished in the hindbrain (Studer et al., 1998), and *Hoxa1*^{null}/*Hoxb1*^{null} double homozygous embryos. The r3 territory of *Hoxa1*^{null} homozygous embryos appeared enlarged when compared to wild-type embryos (Carpenter et al., 1993; Dollé et al., 1993; Studer et al., 1998; compare Fig. 2B,J with Fig. 2A,I), whereas the r5 territory was severely reduced, as suggested by a patchy, dorsally confined, *Krox20* expression at 9.0 dpc (Fig. 2B). Even though *Hoxb1*^{null} homozygous embryos did not show any reduction of r3 and r5 (Goddard et al., 1996; Studer et al., 1996), the combined lack of *Hoxa1* and *Hoxb1* expression further reduced or eliminated the caudal domain of *Krox20* expression (compare Fig. 2B with 2C,D) (Table 2).

Kreisler (*kr)* was used as a marker to assess the status of r5 and r6 (Cordes and Barsh, 1994; Fig. 2E). In *Hoxa1*^{null} homozygous embryos the domain of *kr* expression was reduced (Fig. 2F), reflecting the reduction of the r5 territory, whereas it was not affected in *Hoxb1*^{null} homozygotes (Studer et al., 1996). In this respect *Hoxa1*^{null}/*Hoxb1*$^{3'RARE}$ double homozygotes were not significantly different from *Hoxa1*^{null} homozygotes (Fig. 2G), whereas *Hoxa1*^{null}/*Hoxb1*^{null} double homozygotes showed a further reduction of the *kr* expression domain (Fig. 2H).

The lack of *Hoxb1* expression and the early strong down-regulation of *EphA2*, in both types of double mutants (Studer et al., 1998), raised the question of whether an r4-like territory was formed at all in these embryos. To address this issue *kr* and *Krox20* probes were used simultaneously on 8.75 dpc wild type, *Hoxa1*^{null} homozygous, *Hoxa1*^{null}/*Hoxb1*$^{3'RARE}$ and *Hoxa1*^{null}/*Hoxb1*^{null} double homozygous embryos. In all three

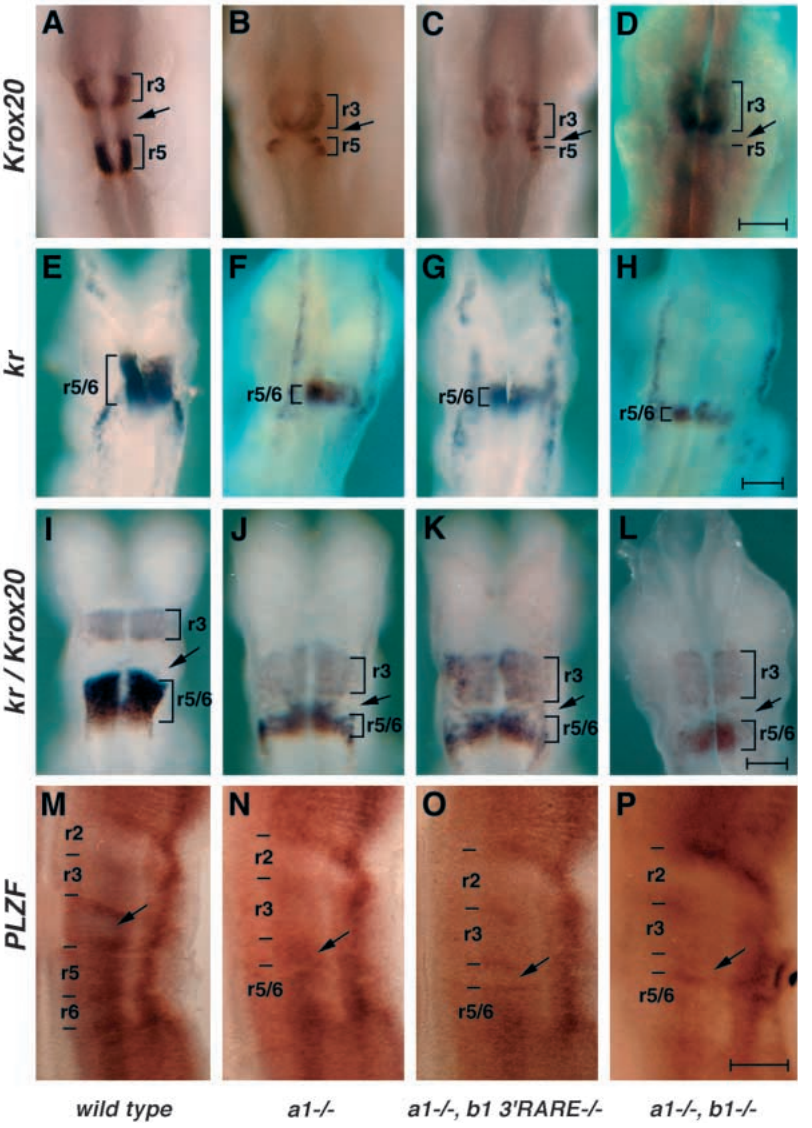

Fig. 2. Molecular markers for the hindbrain segmentation of wild type (A,E,I,M), *Hoxa1* null (B,F,J,N), *Hoxa1*^{null}/*Hoxb1*$^{3'RARE}$ (C,G,K,O) and *Hoxa1/Hoxb1* double null mutants (D,H,L,P). (A-D) Dorsal views of 9.25 dpc embryos immunostained with a *Krox20* antibody (A-C) and hybridised with the *Krox20* antisense RNA(D). (E-H) Dorsal views of 8.75 dpc embryos hybridised with the *kr* antisense RNA. (I-L) Dorsal views of 8.5 dpc (I-K) and 9.0 dpc (L) embryos hybridised with the *Krox20* and *kr* antisense RNAs. (M-P) The right side of flat-mounted hindbrain of 10.5 dpc embryos hybridised with *PLZF* antisense RNA. Arrows indicate the r4 territory; brackets denote rhombomeric territories; short horizontal lines indicate r5 in C and D, and rhombomere boundaries in M-P. Scale bars, 200 μm (A-L), 450 μm (M-P).

Table 1. Summary of nerve defects

Hoxa1$^{3'RARE}$/*Hoxb1*$^{3'RARE}$ double homozygotes (mice at weaning age)	Partially penetrant loss of hyomandibular branch of facial motor nerve.
Hoxa1^{null} homozygotes† (10.5 dpc)	Partially penetrant fusion of V and VII/VIII ganglia; facial and trigeminal motor neurons present in overlapping domains; partially penetrant lack of migrating facial branchiomotor neurons (FBMs); reduced r5-like facial motor axon projections.
Hoxa1^{null}/*Hoxb1*$^{3'RARE}$ double homozygotes (10.5 dpc)	Fully penetrant fusion of V and VII/VIII ganglia; facial and trigeminal motor neurons present in overlapping domains; fully penetrant lack of migrating facial branchiomotor neurons (FBMs); partially penetrant exit of facial motor axons from r2; reduced r5-like facial motor axon projections.
Hoxa1$^{+/-}$/*Hoxb1*$^{null-/-}$* (10.5 dpc)	Partially penetrant loss of IX and X/XI nerves.
Hoxa1^{null}/*Hoxb1*^{null} double homozygotes (10.5 dpc)	V and VII/VIII ganglia either fused or VII/VIII not connected with hindbrain; facial and trigeminal motor neurons present in overlapping domains; reduced neurofilament staining of VII/VIII ganglion and inferior IX, X ganglia; dramatically reduced retrogradely labelled facial motor neurons; lack of r5-like facial motor axon projections.

*Retrograde labelling analysis not performed.
†See also Mark et al. (1993).

types of mutant embryos a similarly reduced r4-like domain persisted (compare Fig. 2I with 2J-L) (Table 2).

To examine segmentation at a later stage, we used the expression of *PLZF*, a gene encoding a zinc-finger protein, as a marker for rhombomeric boundaries (Cook et al., 1995) at 10.5 dpc (Fig. 2M). *Hoxa1*^{null} homozygous embryos showed a reduced r4 territory and a single r5/r6 domain (Fig. 2N), whereas the segmentation pattern of *Hoxb1*^{null} homozygous embryos was normal at this stage (data not shown). A reduced r4-like territory was still formed in both *Hoxa1*^{null}/*Hoxb1*$^{3'RARE}$ double and *Hoxa1*^{null}/*Hoxb1*^{null} double homozygotes (arrows in Fig. 2O,P). Note that *PLZF* expression in this territory was reduced in these mutants, in agreement with its reduction in r4 of *Hoxb1*^{null} homozygotes (data not shown). A further reduction of *PLZF* expression in the caudalmost part of the hindbrain was seen in *Hoxa1*^{null}/*Hoxb1*^{null} double homozygotes (Fig. 2P).

These results suggest that *Hoxa1*^{null}/*Hoxb1*$^{3'RARE}$ and *Hoxa1*^{null}/*Hoxb1*^{null} double homozygous embryos retain a reduced r4-like territory and maintain a hindbrain molecular segmentation pattern similar to that exhibited by *Hoxa1*^{null} homozygotes. They also suggest that some patterning events in the r5/r6 region require the synergistic action of *Hoxa1* and *Hoxb1*.

Synergy of *Hoxa1* and *Hoxb1* in cranial nerve patterning

Whole-mount immunostaining of the cranial nerves and

Table 2. Summary of hindbrain and pharyngeal arch defects

	Hoxa1^{null}* homozygotes	*Hoxa1*^{null}/*Hoxb1*^{RARE}† double homozygotes	*Hoxa1*^{null}/*Hoxb1*^{null}† double homozygotes
Rhombomere 4	Reduced	r4-like territory present	r4-like territory present
Rhombomere 5	Dramatically reduced	Further reduced or absent	Further reduced or absent
Expression of NC markers in second arch (9.25 dpc)			
AP2	Reduced	Further reduced	ND
CRABPI	Reduced	Absent	ND
Second arch at 10.5 dpc	Hypoplastic	Absent	Absent
External ear‡			
Auricle	Normal, occasionally hypoplastic	Absent	Absent
External auditory meatus	Normal	Absent	ND
Middle ear‡			
Tympanic ring	Present, but displaced rostrally	Absent	Absent
Tympanic membrane	Normal	Absent	ND
Stapes	Present, fused to otic capsule	Absent	Absent
Malleus	Present, occasionally hypoplastic	Strongly hypoplastic	Strongly hypoplastic
Incus	Present	Present	Present
Auditory tube	Normal	Absent	ND
Stapedius muscle	Normal	Absent or underdeveloped	ND
Tensor tympani muscle	Normal	Underdeveloped	ND
Inner ear‡			
Vestibular apparatus	Absent or underdeveloped	Absent	Absent
Cochlea	Absent or underdeveloped	Absent	Absent
Styloid process‡	Present, sometimes only distally	Absent	Absent
Hyoid bone‡	Present, slightly deformed	Lesser horns absent, thinner body	Lesser horns absent, thinner body
Stylohyoid muscle‡	Normal	Absent	ND

*As described (Lufkin et al., 1991; Mark et al., 1993, 1995; Dollé et al., 1993; this report).
†This report.
‡At 17.5 dpc and/or 18.5 dpc.
ND Not determined.

associated ganglia and retrograde labelling of the motor neurons were used at 10.5 dpc, to examine the cranial nerve organisation and the segmented pattern of motor neuron axonal projections in *Hoxa1*^{null} homozygotes (Lufkin et al., 1991) as well as in the *Hoxa1*^{null}/*Hoxb1*$^{3'RARE}$ and *Hoxa1*^{null}/*Hoxb1*^{null} double homozygotes. Wild-type embryos as well as *Hoxb1*^{null} and *Hoxb1*$^{3'RARE}$ homozygous embryos from the same colony were used as controls.

Hoxb1^{null} and *Hoxb1*$^{3'RARE}$ homozygotes, immunostained with an anti-neurofilament antibody, were indistinguishable from wild-type embryos (Fig. 3A, and data not shown). The degree to which simple *Hoxa1*^{null} homozygotes were affected was variable, even between the two sides of the same embryo. Six *Hoxa1*^{null} homozygotes were stained. Two embryo sides were indistinguishable from wild type, two embryo sides had the facioacoustic ganglion (VII/VIIIg) well separated from the trigeminal ganglion (Vg), but with a thinner root connecting it to the rhombencephalon (Mark et al., 1993; Fig. 3B), while the remaining sides showed a proximal fusion of the trigeminal with the facioacoustic ganglion (arrow in Fig. 3C). The removal of a single functional *Hoxb1* 3′ RARE in the *Hoxa1*^{null} homozygous background was sufficient to cause a shift to the latter phenotype (five *Hoxa1*$^{null-/-}$/*Hoxb1*$^{3'RARE+/-}$ mutants and one *Hoxa1*^{null}/*Hoxb1*$^{3'RARE}$ double homozygous embryos examined, data not shown).

Three (out of five examined) *Hoxa1*$^{+/-}$/*Hoxb1*$^{null-/-}$ compound mutants lacked unilaterally the proximal part of the glossopharyngeal (IX) nerve (data not shown), and the others unilaterally lacked the proximal part of the vagus (X) and the accessory (XI) nerve as well (Fig. 3D). *Hoxa1*^{null}/*Hoxb1*^{null} double homozygotes (Fig. 3E,F) presented an exacerbation of the abnormal phenotypes shown in Fig. 3C,D. The facioacoustic ganglion was still present and apparently normal in size, but its nerve fibers were thinner and the connection to the rhombencephalon was not always apparent (Fig. 3E,F). The neurofilament staining marking the placode-derived inferior ganglia of the glossopharyngeal and vagus nerves (D'Amico Martel and Noden, 1983) was prominent in the *Hoxa1*^{null} homozygous (Mark et al., 1993; Fig. 3B) and *Hoxa1*^{null}/*Hoxb1*$^{3'RARE}$ double homozygous embryos (data not shown), but significantly reduced in the *Hoxa1*^{null}/*Hoxb1*^{null} double homozygotes (marked with an asterisk, compare Fig. 3B,C with E,F).

The organisation of the motor nuclei and of their axonal projections at 10.5 dpc was analysed using retrograde labelling with lipophilic fluorescent dyes. The close apposition or even apparent fusion of the facial and trigeminal ganglia precluded direct injection of the dye into the ganglia or the nerve roots. Multiple DiO injections were therefore performed, starting distally in the mandibular component of the first arch and moving into the distal part of the trigeminal ganglion. Multiple DiI injections were carried out in a similar manner in the second arch region. In the wild-type embryos all the motor neurons that can be labelled at this stage by retrograde labelling (Marshall et al., 1992) were indeed detected (Fig. 4A,B). Injections in the trigeminal and the facial motor nerves of *Hoxb1*$^{3'RARE}$ homozygous and in the trigeminal motor nerve of *Hoxb1*^{null} homozygous, *Hoxa1*^{null}/*Hoxb1*$^{3'RARE}$ and *Hoxa1*^{null}/*Hoxb1*^{null} double homozygous embryos (Studer et al., 1996) resulted in a pattern of labelled cell-bodies and axons similar to that of wild-type embryos (Fig. 4D-R; and data not shown).

The *Hoxa1*^{null} homozygotes used in this study (Lufkin et al., 1991), not previously analysed by DiI/DiO motorneuron tracing, showed multiple defects in the motor neuron axonal projections and the location of cell bodies (Fig. 4D-I). The presumptive r3 territory appeared to host motor neurons projecting not only towards the trigeminal ganglion through the r2 exit point but also towards the facial ganglion through multiple and ectopic r3 exit points. The degree of mixing

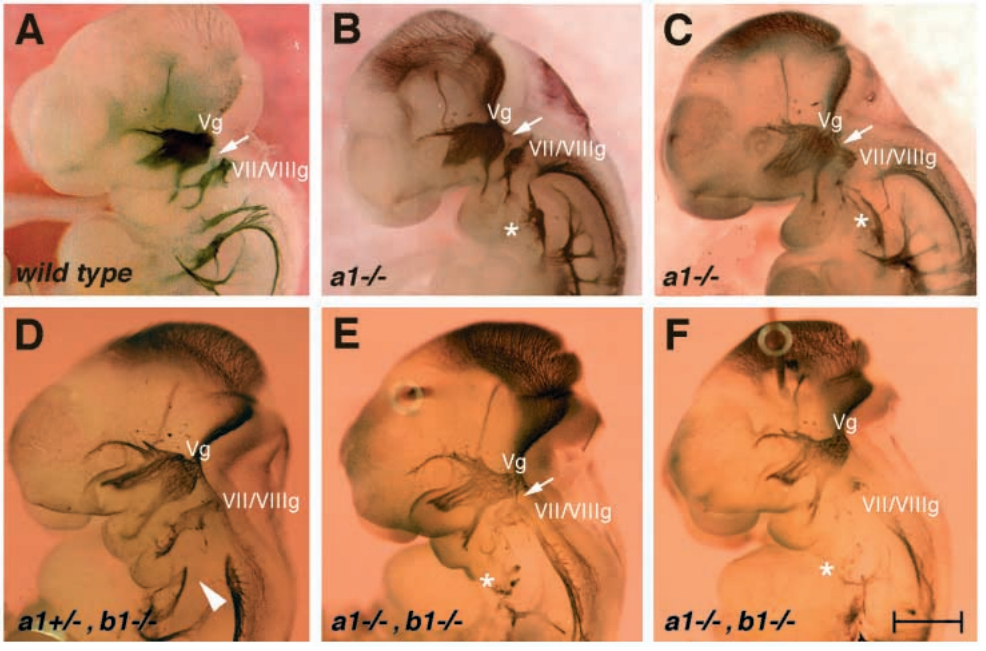

Fig. 3. Neurofilament immunostaining of the cranial nerves of wild type and mutant embryos at 10. 5 dpc (lateral views). (A) Wild-type embryo; note the well individualised (arrow) trigeminal (Vg) and facioacoustic (VII/VIIIg) ganglia. (B) *Hoxa1* null mutant presenting a weak phenotype; Vg and VII/VIIIg are still separated (arrow). (C) Phenotype exhibited by the majority of *Hoxa1* null mutants and all *Hoxa1*^{null}/*Hoxb1*$^{3'RARE\ +/-\ or\ -/-}$ embryos. Note the fusion between the Vth and VII/VIIIth ganglia (arrow). (D) *Hoxa1*$^{+/-}$/*Hoxb1*^{null} mutants. Note the lack of the IX,X and XI nerves (arrowhead). (E,F) *Hoxa1/Hoxb1* double null mutants. Note the weak staining of the VII/VIIIth ganglion and of its projections. In these mutants this ganglion is either fused (arrow) with the Vth (E), or individualised but not connected to the rhombencephalon (F). Asterisks denote the abnormal inferior ganglia of the IXth and Xth nerves in *Hoxa1* null mutants (B,C) and *Hoxa1/Hoxb1* double null mutants (E,F). Scale bar, 1 mm.

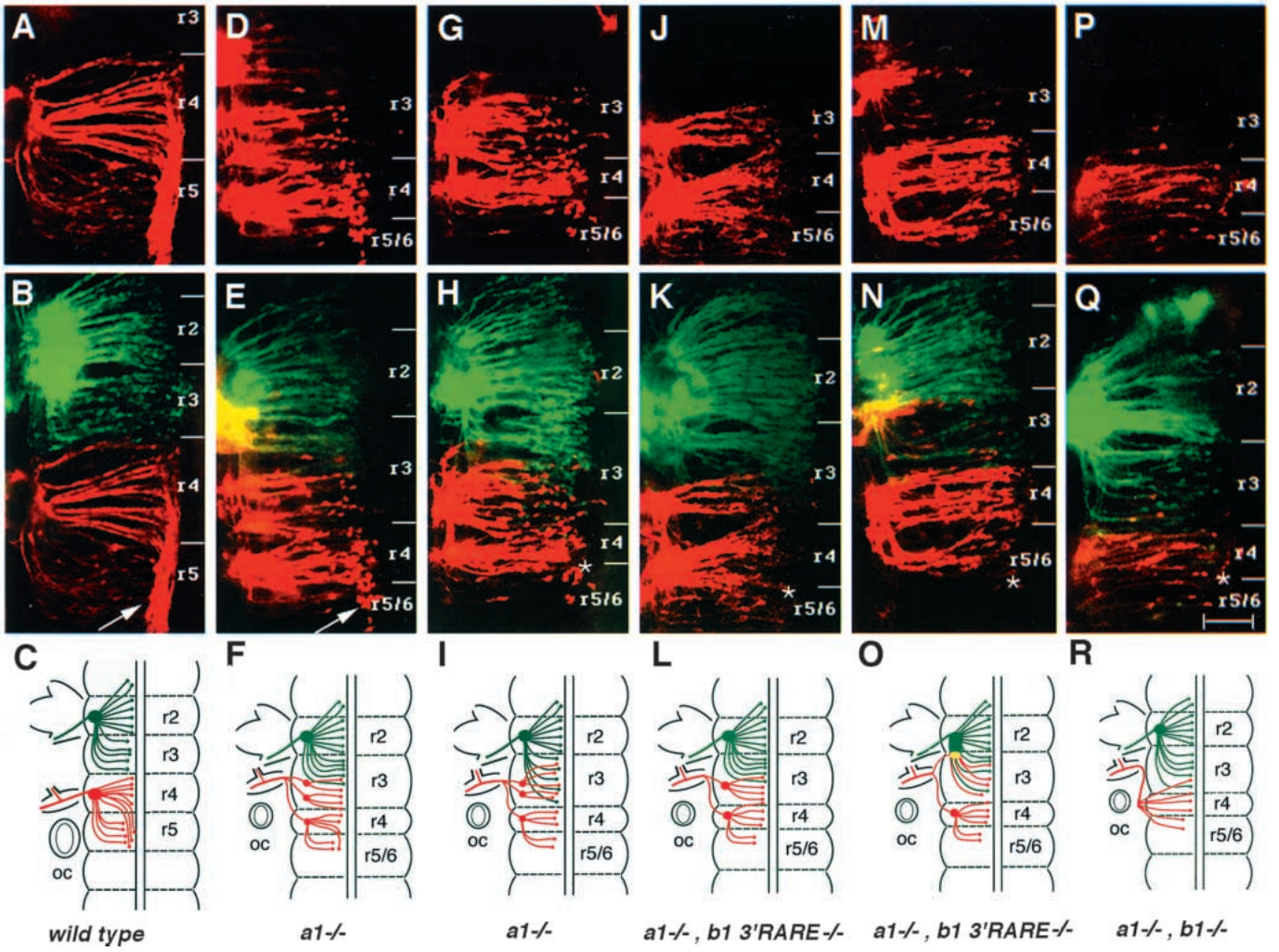

Fig. 4. Retrograde labelling of facial and trigeminal motor nerves. Retrograde labelling with DiI (red) of the facial motor nerve alone (A,D,G,J,M,P) and combined with the retrograde labelling of the trigeminal motor nerve with DiO (green) (B,E,H,K,N,Q) at 10.5 dpc. Overlaps of the tracings appear as yellow. (C,F,I,L,O,R) Interpretative diagrams of the injection results depicted directly above them. Representative specimens of wild type (A-C), *Hoxa1* null mutants (D-I), *Hoxa1*^{null}/*Hoxb1*$^{3'RARE}$ double mutants (J-O) and *Hoxa1/Hoxb1* double null mutants are shown. Arrows in B and E denote the migrating facial branchiomotor neurons (FBM) and the asterisks (H,K,N,Q) their absence. oc, otocyst. Bar, 100 μm.

between the facial and trigeminal motor neurons varied from minimal (Fig. 4D-F) to extensive (Fig. 4G-I). In wild-type embryos the facial branchiomotor neurons (FBMs) are formed in r4 and, subsequently, migrate into r5 and r6 along the lateral border of the floorplate (Studer et al., 1996; arrow in Fig. 4B). The r4 territory of the *Hoxa1*^{null} homozygotes produced motor neurons that projected normally, but failed to migrate caudally into r5 in some (5/8) mutants (compare Fig. 4A,B and D,E with G,H), thus presenting a *Hoxb1*^{null} homozygous phenotype (Goddard et al., 1996; Studer et al., 1996). Furthermore, there was a considerable loss, but not elimination, of motor neurons with axonal projections typical of r5 (i.e. exiting from the vestigial r4) (compare Fig. 4A,B with D,E,G,H).

To determine whether the combined lack of *Hoxa1* and *Hoxb1* expression in the hindbrain resulted in an abnormal motor neuron phenotype stronger than that of single *Hoxa1*^{null} and *Hoxb1*^{null} homozygotes, we analysed the *Hoxa1*^{null}/*Hoxb1*$^{3'RARE}$ (Fig. 4J-O) and *Hoxa1*^{null}/*Hoxb1*^{null} double homozygotes (Fig. 4P-R). *Hoxa1*^{null}/*Hoxb1*$^{3'RARE}$ double homozygotes were more severely affected than *Hoxa1*^{null} homozygotes, since migrating FBM motor neurons were always lacking (Fig. 4J-O) and in two out of six examined *Hoxa1*^{null}/*Hoxb1*$^{3'RARE}$ double homozygotes, r3-residing facial motor axons turned rostrally and exited abnormally through the r2 exit point (Fig. 4M-O). *Hoxa1*^{null}/*Hoxb1*^{null} double homozygotes presented a more abnormal phenotype since facial motor neurons were scarce and appeared to exit randomly from the neural tube without fasciculating towards distinct exit points (Fig. 4P-R). The reduced number of motor neurons was in agreement with the scarcity of facial nerve fibers in the periphery (Fig. 3E,F).

The neurofilament staining and the dye injection results (summarised in Table 1) indicate that *Hoxa1* and *Hoxb1* synergise in patterning the VIIth through XIth cranial nerves. Moreover, the strength of the neurofilament staining and the

number of retrogradely labelled motor neurons appear to be dramatically reduced in the *Hoxa1*^{null}/*Hoxb1*^{null} double homozygotes, as compared to the *Hoxa1*^{null}/*Hoxb1*$^{3'RARE}$ double homozygotes.

Changes in the NC cells migrating into the second pharyngeal arch correlate with its subsequent involution

The combined changes in the patterning and molecular identity of the r4 territory in both *Hoxa1*^{null}/*Hoxb1*$^{3'RARE}$ double homozygotes and *Hoxa1*^{null}/*Hoxb1*^{null} double homozygotes (see above, and Studer et al., 1998), prompted us to examine the status of the NC cells of this territory. To that end we used *AP2* and *CRABPI* probes in whole-mount in situ hybridisations. *AP2* is a transcription factor expressed in NC cells and their major derivatives (Mitchell et al., 1991). The functional inactivation of this gene results in severe craniofacial defects, demonstrating its essential role in NC development (Schörle et al., 1996; Zhang et al., 1996). *CRABPI*, a RA binding protein, is expressed in both the neural epithelium and the migrating NC cells, but not in paraxial mesodermal cells (Ruberte et al., 1992; Maden et al., 1992).

In 9.25 dpc wild-type embryos, both *AP2* (Fig. 5A) and *CRABPI* (Fig. 5D) were expressed in the three distinct streams of cells migrating into the first, the second and the third pharyngeal arches (Lumsden et al., 1991). The reduced intensity of *AP2* staining in both *Hoxa1*^{null} homozygous and *Hoxa1*^{null}/*Hoxb1*$^{3'RARE}$ double homozygous embryos (Fig. 5B,C) as compared to wild-type embryos (Fig. 5A), suggests a decrease in the amount of NC cells migrating into the second branchial arch of these mutants. However, whereas *Hoxa1*^{null} homozygotes exhibited a strongly reduced, but still detectable, expression of *CRABPI* (compare Fig. 5E with F), no *CRABPI* expression could be detected in the second arch of the *Hoxa1*^{null}/*Hoxb1*$^{3'RARE}$ double homozygous embryos. It should be noted that *CRABPI* expression was normal in the second pharyngeal arch of *Hoxb1*^{null} homozygotes (Fig. 5G) and that, at this stage (9.25 dpc), there are no obvious morphological differences in the region of the pharyngeal arches between wild-type embryos, *Hoxa1*^{null} homozygotes and *Hoxa1*^{null}/*Hoxb1*$^{3'RARE}$ double homozygotes (Fig. 5D-F). In contrast, the second pharyngeal arch of *Hoxa1*^{null}/*Hoxb1*^{null} double homozygotes was not identifiable at 9.5 dpc (compare Fig. 5G with H).

To look for the second pharyngeal arch at later stages (10.5 dpc), we used both a *PLZF* probe, as this gene is expressed in the mesenchyme of the first and second pharyngeal arches (Cook et al., 1995), and scanning electron microscopy (SEM). A clear, stepwise loss of *PLZF* expression was observed in the second pharyngeal arch when *Hoxa1*^{null} homozygotes (Fig. 5J), *Hoxa1*^{null}/*Hoxb1*$^{3'RARE}$ double homozygotes (Fig. 5K) and *Hoxa1*^{null}/*Hoxb1*^{null} double homozygotes (Fig. 5L) were compared to wild-type embryos (Fig. 5I). This reflected the dramatic reduction of the second pharyngeal arch in both types of double mutants, as observed by SEM and paralleled the reduction in *CRABPI* expression in the second arch. The second pharyngeal arch was hypoplastic in *Hoxa1*^{null} homozygotes and was replaced by a flattened surface in both types of double mutants (Fig. 6A-C and data not shown). It is worth noting that aplasia of the second arch was also evident in both *Hoxa1*$^{null-/-}$/*Hoxb1*$^{+/-}$ and *Hoxa1*$^{null-/-}$/*Hoxb1*$^{3'RARE+/-}$ embryos, albeit with a lower penetrance in the latter case (data not shown).

Thus, the combined lack of *Hoxa1* and *Hoxb1* expression in the hindbrain of *Hoxa1*^{null}/*Hoxb1*$^{3'RARE}$ and *Hoxa1*^{null}/*Hoxb1*^{null} double homozygous embryos results in molecular alterations of the second arch NC cells (summarised in Table 2) with a subsequent early disruption of second arch development. Note that it is not excluded that migratory defects of the second arch NC cells could also contribute to this phenotype.

Full disruption of ear development and lack of second arch-derived skeletal elements in the *Hoxa1*^{null}/*Hoxb1*$^{3'RARE}$ double homozygotes

The external ear develops from the first and second pharyngeal

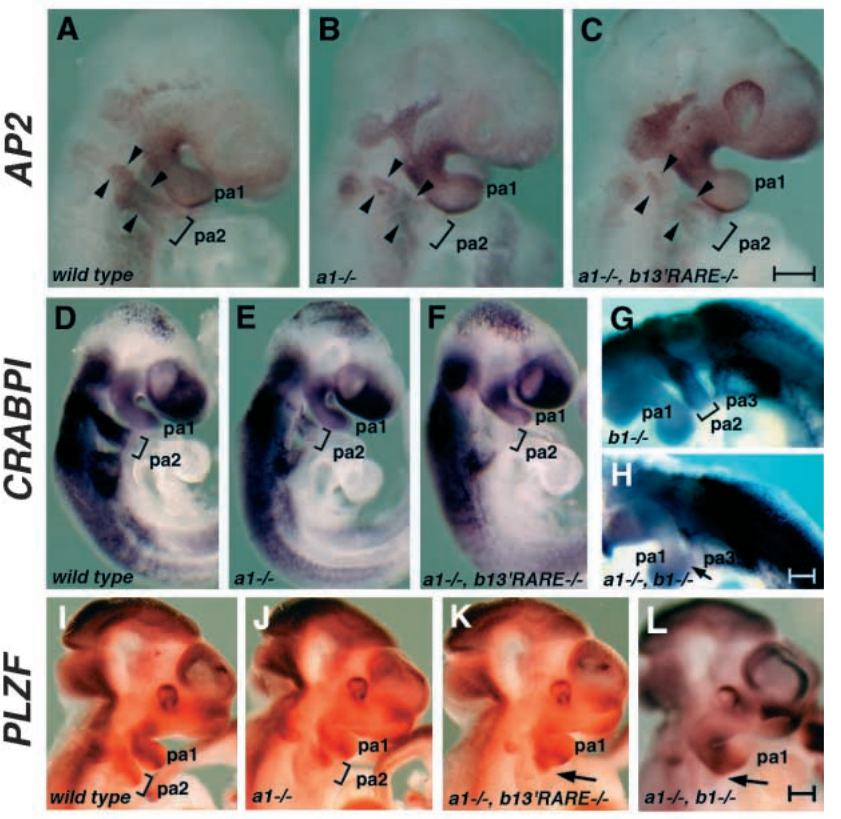

Fig. 5. Expression of molecular markers in the pharyngeal arches. Wild type (A,D,I), *Hoxa1* null mutants (B,E,J), *Hoxb1* null mutants (G), *Hoxa1*^{null}/*Hoxb1*$^{3'RARE}$ double mutants (C,F,K) and *Hoxa1/Hoxb1* double null mutants. (H,L) were hybridised with an *AP2* antisense probe at 9.25 dpc (A-C), *CRABPI* at 9.25 (D-F) and 9.5 (G,H) and *PLZF* at 10.5 dpc (I-L). Arrowheads in (A-C) mark *AP2*-positive cells in the second pharyngeal arch (pa2). Brackets mark the second arch in wild type (A,D,I), *Hoxa1* null mutants (B,E,J) and *Hoxb1* (G) null mutants. Arrows mark the aplasia of the second arch in *Hoxa1*^{null}/*Hoxb1*$^{3'RARE}$ double (K) and *Hoxa1/Hoxb1* double null mutants (H,L). Bars, 100 μm (A-H), 200 μm (I-L).

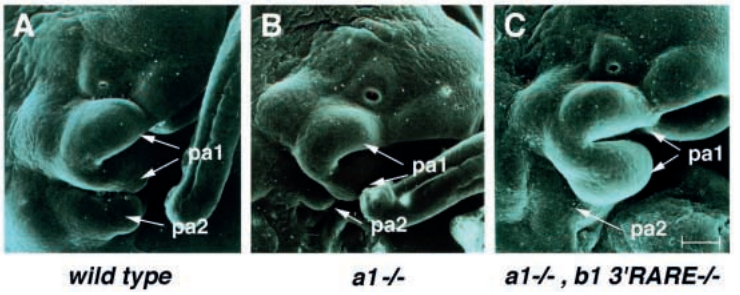

Fig. 6. Scanning electron microscopy of the facial region at 10.5 dpc. Arrows mark the first (pa1) and second pharyngeal (pa2) arches. Note the increasing reduction of the second pharyngeal arch from the wild type (A) to *Hoxa1* null mutants (B) to *Hoxa1*^{null}/*Hoxb1*$^{3'RARE}$ double mutants (C). Bar, 200 μm.

arches and also from the first pharyngeal cleft. In *Hoxa1*^{null} homozygous newborns the auricle is formed but occasionally hypoplastic (Lufkin et al., 1991; data not shown). Strikingly, the auricle is missing, in the *Hoxa1*^{null}/*Hoxb1*$^{3'RARE}$ double homozygotes (Fig. 7A,B), whereas it was rudimentary in *Hoxa1*$^{null-/-}$/*Hoxb1*$^{3'RARE+/-}$ mutants (data not shown). The external auditory meatus, which is derived from the first pharyngeal cleft, was also not formed in the *Hoxa1*^{null}/*Hoxb1*$^{3'RARE}$ double homozygotes, in contrast to *Hoxa1*^{null} and *Hoxb1*^{null} homozygotes (Fig. 7C-E and data not shown).

As the middle ear is derived from the first and second pharyngeal arches as well as from the first pharyngeal pouch, we also examined its development in *Hoxa1*^{null}/*Hoxb1*$^{3'RARE}$ double homozygous fetuses. In *Hoxa1*^{null} homozygotes the tympanic ring, a first arch NC-derived middle ear ossicle, was always fully formed, but rostrally displaced (Lufkin et al., 1991; Fig. 7F). In contrast, it was never present in *Hoxa1*^{null}/*Hoxb1*$^{3'RARE}$ double hoozygotes (Fig. 7F) and only partially formed in *Hoxa1*$^{null-/-}$/*Hoxb1*$^{3'RARE+/-}$ fetuses (data not shown). The tympanic membrane was also lacking in double mutant fetuses (data not shown). The malleus, which is derived from the NC of the first arch, was either correctly formed or had a slightly smaller neck and processus brevis (in 7/14 middle ears examined) in *Hoxa1*^{null} homozygotes, but was markedly reduced in *Hoxa1*^{null}/*Hoxb1*$^{3'RARE}$ double homozygotes (Mark et al., 1995; Fig. 7F). The tensor tympani muscle, which attaches to the cartilaginous part of the auditory

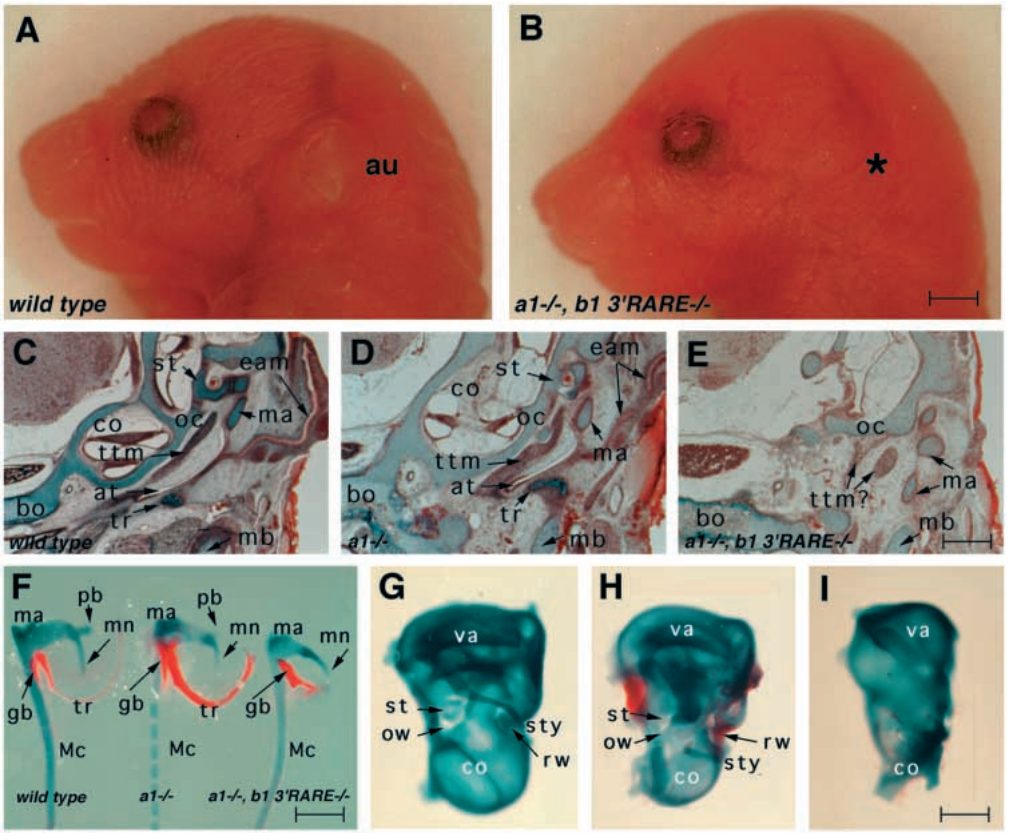

Fig. 7. Disruption of ear development. (A,B) The auricle (au) is readily visible in wild-type newborns (A) but is missing (asterisk) in *Hoxa1*^{null}/*Hoxb1*$^{3'RARE}$ double mutant newborns (B). (C-E) Transverse histological sections of wild type (C), *Hoxa1* null (D) and *Hoxa1*^{null}/*Hoxb1*$^{3'RARE}$ double mutants (E), 17. 5 dpc embryos. Note the absence, specifically in the double mutants, of the external auditory meatus (eam), the stapes (st), the auditory tube (at), the tympanic ring (tr) and the hypoplasia of the tensor tympani muscle (ttm). Note also the fusion of the stapes with the otic capsule (oc) in the *Hoxa1* null mutants (D). ma, malleus; co, cochlea; bo, basioccipital bone; mb, mandible; Mc, Meckel's cartilage. (F) Dissected middle ear ossicles from wild-type and mutant newborns. Note the lack of the tympanic ring (tr) in the *Hoxa1*^{null}/*Hoxb1*$^{3'RARE}$ double mutants, and the increasing aplasia of the malleus (ma) from the wild type to the *Hoxa1* null mutant to the *Hoxa1*^{null}/*Hoxb1*$^{3'RARE}$ double mutant newborns. pb, processus brevis of the malleus; mn, manubrium of the malleus; gb, gonial bone. The Meckel's cartilage of the *Hoxa1* mutant was cut during dissection, and hence it is represented here with a dashed line. (G,H,I) The medial surface of the right inner ear of a wild type (G), a mildly affected *Hoxa1* homozygote (H) and a typical *Hoxa1*^{null}/*Hoxb1*$^{3'RARE}$ double mutant newborn (I) are shown. Note the absence of the cochlea (co), the styloid (sty), the aplasia of the vestibulary apparatus (va) and the lack of any fenestration in the inner ear of the *Hoxa1*^{null}/*Hoxb1*$^{3'RARE}$ double mutant. ow, oval window; rw, round window. Bars, 2 mm (A,B), 250 μm (C-F) and 400 μm (G-I).

tube and the handle of the malleus, was also underdeveloped in the *Hoxa1*^{null}/*Hoxb1*$^{3'RARE}$ double homozygotes, but not in *Hoxa1*^{null} homozygotes (Mark et al., 1995; compare Fig. 7C,D with E). This is not surprising, given the obliteration of the auditory tube and the underdeveloped malleus in these embryos. The incus did not appear to be affected in the examined *Hoxa1*^{null} homozygotes and *Hoxa1*^{null}/*Hoxb1*$^{3'RARE}$ double homozygotes. The stapes, a second arch-derived element, is normally attached by its footplate to the labyrinth membrane lining the oval window (Fig. 7C) and is associated with the stapedius muscle. In the examined *Hoxa1*^{null} homozygotes, both the stapedius muscle and the stapes were present, the latter being fused to the otic capsule (Mark et al., 1993; Fig. 7D). Strikingly, in *Hoxa1*^{null}/*Hoxb1*$^{3'RARE}$ double homozygotes the oval window was not formed (compare Fig. 7I with H,G) and the stapes was lacking (compare Fig. 7E with C,D) whereas the stapedius muscle is underdeveloped or lacking (data not shown).

The inner ear develops from the ectodermal otic placode, which appears bilaterally alongside r5 and r6 at the time of neural tube closure (Noden and Van de Water, 1986; Keynes and Lumsden, 1990). It has been suggested that inductive signals emanating from the rhombencephalon are crucial for early induction of the otic placode and subsequent differentiation of the otocyst. Inner ear malformations in the cochlea and the vestibular apparatus were variable in *Hoxa1*^{null} homozygotes (Fig. 7H,I) but fully penetrant in *Hoxa1*^{null}/*Hoxb1*$^{3'RARE}$ double homozygotes (Fig. 7I). Five out of 14 *Hoxa1*^{null} homozygous inner ears examined still had a partially formed cochlea and six had recognisable semicircular canals (Fig. 7H), whereas these structures invariably fail to form in *Hoxa1*^{null}/*Hoxb1*$^{3'RARE}$ double homozygotes (12 inner ears examined) (Fig. 7I).

The styloid process is a second-arch skeletal element (Noden, 1988; Köntges and Lumsden, 1996). In the *Hoxa1*^{null} homozygotes, the styloid was either correctly formed (9/14 inner ears examined, data not shown) or at least its distal part was present (Fig. 7G,H), whereas it was not identifiable in the *Hoxa1*^{null}/*Hoxb1*$^{3'RARE}$ double homozygotes (Fig. 7I). The lesser horns and cranial part of the body of the hyoid bone are formed by NC cells of the second arch, whereas its greater horns and the rest of its body are derived from the third arch (Noden, 1988; Köntges and Lumsden, 1996). In the *Hoxa1*^{null} homozygous fetuses, the hyoid bone was always correctly formed (Lufkin et al., 1991), although it appeared slightly twisted sometimes (Fig. 8B). The hyoid bone of *Hoxa1*^{null}/*Hoxb1*$^{3'RARE}$ double homozygotes was always missing its second arch-derived elements, as indicated by the lack of the lesser horns and a thinning of the body. The greater horns were fused dorsally with the thyroid cartilage (Fig. 8C). No defects in bones of mesodermal origin (occipital, intraparietal and cervical) were observed in *Hoxa1*^{null}/*Hoxb1*$^{3'RARE}$ double homozygotes, other than those already described for *Hoxa1*^{null} homozygotes (Lufkin et al., 1991). The skeletons of *Hoxa1*^{null}/*Hoxb1*^{null} double homozygotes showed additional mild abnormalities in the occipital/cervical region only (data not shown).

No ear or pharyngeal arch defects have been reported in *Hoxb1*^{null} homozygotes (Goddard et al., 1996; Studer et al., 1996). The full disruption of ear development and the loss of all second arch-derived skeletal elements in

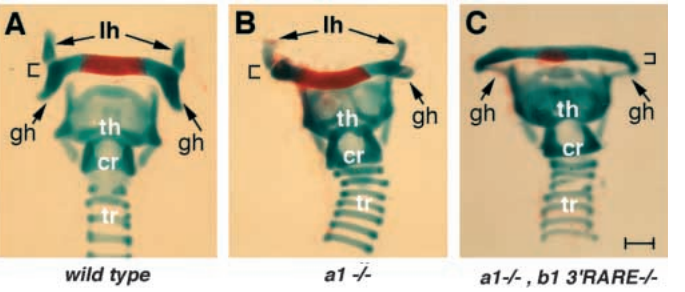

Fig. 8. Morphology of the hyoid bone of newborns. All the elements of the hyoid bone are present in wild-type (A) and *Hoxa1* null mutant newborns (B), whereas its lesser horns (lh) are lacking, its body is thinner and the greater horns (gh) are fused dorsally with the thyroid cartilage (th) in *Hoxa1*^{null}/*Hoxb1*$^{3'RARE}$ double mutant newborns. The right side greater horn in (B) is hidden behind the body of the bone. Brackets indicate the thickness of the body of the hyoid bone. cr, cricoid cartilage; tr, trachea. Bar, 75 μm.

Hoxa1^{null}/*Hoxb1*$^{3'RARE}$ double homozygotes correlate with the involution of the second pharyngeal arch and additional patterning defects in the hindbrain of these mutants (summarised in Table 2). Unexpectedly, defects in first arch-derived elements of *Hoxa1*^{null}/*Hoxb1*$^{3'RARE}$ and *Hoxa1*^{null}/*Hoxb1*^{null} double homozygous fetuses have been observed (summarised in Table 2), most notably the lack of the tympanic ring. Additional skeletal defects of mesodermal origin have been detected only in the *Hoxa1*^{null}/*Hoxb1*^{null} double homozygotes fetuses, which suggest that mesodermal expression of *Hoxb1* is not abolished in the *Hoxa1*^{null}/*Hoxb1*$^{3'RARE}$ double homozygous embryos.

DISCUSSION

In this study we have examined the synergistic function of *Hoxa1* and *Hoxb1* in patterning the hindbrain, the cranial nerves and the pharyngeal arches. Lowering the response of both genes to endogenous retinoids leads to minor, not fully penetrant defects in the development of the facial nerve. In contrast, we have unveiled extensive synergy between the products of the two genes by generating *Hoxa1*^{null}/*Hoxb1*$^{3'RARE}$ and *Hoxa1*^{null}/*Hoxb1*^{null} double homozygotes. Interestingly, these mutants show additional molecular changes in the r4-r6 hindbrain region and in the second pharyngeal arch NC cells, resulting in early disruption of the second arch development, subsequent loss of its derivatives, full disruption of ear development and further patterning defects of the cranial nerves (summarised in Tables 1 and 2).

Overlapping functions of *Hoxa1* and *Hoxb1* in hindbrain patterning

Detailed analysis of the rhombencephalon of the *Hoxa1*^{null} homozygotes used in this study by three-dimensional reconstructions (Lufkin et al., 1991) has shown the presence of a single enlarged rhombomeric structure in place of the wt r4/r5/r6 distinct rhombomeres (Mark et al., 1993). However, further analysis suggested that this structure was molecularly divided in distinct territories corresponding to a reduced r4, the

remnant of r5, and r6 (Dollé et al., 1993). Using molecular markers, we have analysed *Hoxa1^{null}/Hoxb1$^{3'RARE}$* homozygotes and *Hoxa1^{null}/Hoxb1^{null}* double homozygotes in order to determine whether the combined lack of *Hoxa1* and *Hoxb1* expression in the hindbrain leads to further alterations of the segmentation pattern.

The caudal domain of *Krox20* expression is further reduced or completely eliminated in *Hoxa1^{null}/Hoxb1$^{3'RARE}$* homozygotes and *Hoxa1^{null}/Hoxb1^{null}* double homozygotes. This implies that the establishment of *Krox20* expression in r5 may depend on signals from r4 and/or the presence of *Hoxa1* and *Hoxb1* in the presumptive r5 of the presomitic embryo. The combined r5/r6 territory does not appear to be significantly altered in the *Hoxa1^{null}/Hoxb1$^{3'RARE}$* homozygotes, as assessed by *kr* and *PLZF* expression, when compared to that of *Hoxa1^{null}* homozygotes. However, this territory is further reduced in *Hoxa1^{null}/Hoxb1^{null}* double homozygotes. As *Hoxb1* mesodermal expression is not abolished (Studer et al., 1998; see also above) in the *Hoxa1^{null}/Hoxb1$^{3'RARE}$* double homozygotes, this difference could reflect a mesodermal contribution of *Hoxb1* in patterning the presumptive r5/r6 region of the neural plate via vertical inductive signals (Frohman et al., 1990).

A population of cells molecularly distinct from either r3 or r5/r6 territories (see above) is present at 8.75 dpc and maintained up to 10.5 dpc in the absence of *Hoxa1* and *Hoxb1*. Interestingly, the size of this r4-like segment, as assessed by *PLZF* staining at 10.5 dpc, is not further reduced in both double mutants, as compared to *Hoxa1^{null}* homozygotes. *Hoxb2* is the only other *Hox* gene strongly expressed in r4 (Wilkinson et al., 1989b) and it is likely to be involved, in combination with *Hoxa1* and *Hoxb1*, in establishment/maintenance of this rhombomere, as only its late phase of expression is dependent on *Hoxb1* (Maconochie et al., 1997). It is noteworthy that the *Hoxa1^{null}* homozygotes generated by Chisaka et al. (1992) lack segmentation in the hindbrain. A key difference may lie, in the latter study, in the retention of a truncated *Hoxa1* protein, encompassing the N-terminal of the protein but lacking the homeobox (La Rosa and Gudas, 1988). This truncated protein may compete for common interacting factors with other *Hox* proteins, particularly with Hoxb1 and Hoxb2, thus exacerbating the *Hoxa1^{null}* homozygous phenotype. In this respect, it is noteworthy that external and middle ear defects reported for the *Hoxa1^{null}* homozygotes generated by Chisaka et al. (1992) are not observed in the *Hoxa1^{null}* homozygotes used here (Lufkin et al., 1991), while they are present in the *Hoxa1^{null}/Hoxb1$^{3'RARE}$* and *Hoxa1^{null}/Hoxb1^{null}* double homozygotes.

It has been suggested that inductive signals emanating from the rhombencephalon are crucial for the early induction of the otic placode and differentiation of the otocyst (Noden and Van De Water, 1986). In *Hoxa1^{null}* homozygotes, normal development of the inner ear is affected but the penetrance of the defects is not complete, indicating that early inductive events and/or subsequent morphogenesis are not fully disrupted. Consistent with the data indicating that *Hoxa1* and *Hoxb1* synergise in patterning the r4-r6 region, we find here that the disruption of inner ear development is fully penetrant in the *Hoxa1^{null}/Hoxb1$^{3'RARE}$* double homozygotes.

In summary, the *Hoxa1^{null}* segmentation defects do not appear to be greatly exacerbated in the presented double mutants, apart from further reduction or loss of the caudal *Krox20* expression domain. However, the specific loss of *EphA2* expression at the 0- to 2-somite-stage in both types of double mutants (Studer et al., 1998) suggests a change in the identity of the prospective r4 territory. A further reduction of the r6 territory is seen specifically in the *Hoxa1^{null}/Hoxb1^{null}* double homozygotes. Taken together, these results demonstrate that abrogation of *Hoxb1* expression in a *Hoxa1^{null}* homozygous background does not further affect segmentation but alters the identity of r4 and repatterns the r5/r6 territory. Thus, *Hoxa1* and *Hoxb1* appear to functionally synergise for r4 specification but not in hindbrain segmentation.

Hoxa1 and *Hoxb1* synergize in patterning the cranial nerves

Results from the analysis of the *Hoxa1^{null}* and *Hoxb1^{null}* homozygotes have implicated these paralogs in distinct aspects of cranial nerve development (Carpenter et al., 1993; Mark et al., 1993; Goddard et al., 1996; Studer et al., 1996). The analysis of *Hoxa1$^{3'RARE}$/Hoxb1$^{3'RARE}$*, *Hoxa1^{null}/Hoxb1$^{3'RARE}$* and *Hoxa1^{null}/Hoxb1^{null}* double homozygotes indicates that *Hoxa1* and *Hoxb1* synergise in patterning the cranial nerves (Table 1).

The number of *Hoxa1$^{3'RARE}$/Hoxb1$^{3'RARE}$* double homozygotes lacking specifically the hyomandibular branch of the facial motor nerve correlates well with the percentage of embryos exhibiting a dorsally reduced *Hoxb1* expression at 9.5 dpc (Studer et al., 1998), suggesting a causal relationship. This may also imply differential requirements in levels of *Hox* gene expression for the development of different branches of the facial nerve.

The *Hoxa1^{null}* homozygotes further analysed here (Lufkin et al., 1991) show extensive intermixing of V and VII/VIII nerve efferent cell bodies, as do the *Hoxa1^{null}* homozygotes generated by Chisaka et al. (1992) (Carpenter et al., 1993). The present analysis, performed at an earlier stage, shows in addition that the VII/VIII nerve efferent axons have multiple exit points rostral to the normal r4 exit point. The intermixing of V and VII/VIII nerve efferent cell bodies and their abnormal axonal projections in both *Hoxa1^{null}* homozygotes (Carpenter et al., 1993; this study) might be due to extensive intermixing of r3 and r4 cells, and impaired segmental distribution of NC leading to ectopic exit points able to attract outgrowing motor axons (Niederlander and Lumsden, 1996). This could result from early impaired cell lineage restriction in these mutants (Guthrie and Lumsden, 1991; Guthrie et al., 1993). The apparently normal number of motor neurons labelled by dye injections in *Hoxa1^{null}* homozygotes suggests that the reduction or loss of the facial nucleus, detected in these mutants (Lufkin et al., 1991; Mark et al., 1993), occurs at a later stage, possibly due to degenerative processes. The variability seen in the generation of migrating FBM motorneurons in the *Hoxa1^{null}* homozygotes may reflect lower levels of *Hoxb1* expression in these mutants (Carpenter et al., 1993; Dollé et al., 1993), and subsequently stochastic processes of FBM specification. Accordingly, we have never detected such neurons in *Hoxa1^{null}/Hoxb1$^{3'RARE}$* homozygotes, which do not express *Hoxb1* in the hindbrain (Studer et al., 1998).

The reduced number of r5-like motor neurons in the *Hoxa1^{null}* homozygotes and *Hoxa1^{null}/Hoxb1$^{3'RARE}$* double homozygotes is not surprising given the drastic reduction of

this territory indicated by molecular and histological criteria (Dollé et al., 1993; Mark et al., 1993; see above). On the other hand, some of these neurons may reside in r6 and are now able to project towards r4 due to the reduction of r5 (see also Carpenter et al., 1993; these *Hoxa1*^{null} homozygotes lack r5 completely). This has been shown to occur in the *Krox20* null mutants (Schneider-Maunoury et al., 1997).

The occurrence of facial motor axons exiting from r2 in the *Hoxa1*^{null}/*Hoxb1*$^{3'RARE}$ double homozygotes, may indicate a more extensive rostral spread of r4-like motor neuron precursors in these mutants. It cannot be excluded that molecular changes in the neuroepithelium, similar to those occurring in *Hoxa2* null mutants (Taneja et al., 1996; Gavalas et al., 1997), contribute to mis-direction of the motor axons. However, extensive mixing of r3 and r4 cells in *Hoxa1*^{null} homozygotes and, perhaps to a higher degree, in *Hoxa1*^{null}/*Hoxb1*$^{3'RARE}$ double homozygotes, seems sufficient to account for the cranial nerve abnormal phenotype. It should be noted that, despite the full penetrance of the fused ganglia phenotype, the trigeminal and facioacoustic ganglia retain their selective wiring.

The combination of *Hoxa1*^{null} and *Hoxb1*^{null} mutations results in further nerve defects. The *Hoxa1*$^{+/-}$/*Hoxb1*$^{null-/-}$ mutants fail in many instances to form the proximal part of the IX and X/XI nerves. These defects are reminiscent of those in the *Hoxa1*^{null} homozygotes, and may be due to failure of the r6-r8 neurogenic crest cells to form the superior ganglia (Mark et al., 1993, and references therein). This further supports the notion that, beyond synergising in r4 patterning, *Hoxa1* and *Hoxb1* synergise also in patterning the caudal hindbrain.

Earlier studies have suggested that the placode-derived part of the trigeminal ganglion is necessary for trigeminal motor axon outgrowth (Moody and Heaton, 1983). The dramatically reduced number of facial motor neurons and reduced neurofilament staining in the *Hoxa1*^{null}/*Hoxb1*^{null} double homozygotes may be due to additional patterning defects of the facioacoustic ganglion. Interestingly, these defects are not present in the *Hoxa1*^{null}/*Hoxb1*$^{3'RARE}$ double homozygotes, despite the loss of *Hoxb1* expression in the hindbrain. This suggests that *Hoxb1* expression in other tissues (e.g. mesoderm, pharyngeal endoderm) of these mutants is not abolished, rescuing the above defects. In support of this hypothesis, *Hoxa1*^{null}/*Hoxb1*^{null} double homozygotes show mesodermal defects not present in the *Hoxa1*^{null}/*Hoxb1*$^{3'RARE}$ double homozygotes.

In conclusion, our results (Table 1) indicate that *Hoxa1* and *Hoxb1* synergise in patterning the cranial nerves VII through XI. *Hoxa1*$^{+/-}$/*Hoxb1*$^{null-/-}$ mutants show malformations in cranial nerves IX through XI not present in either *Hoxa1*^{null} hetrozygotes or *Hoxb1*^{null} homozygotes. Defects that are not fully penetrant in the *Hoxa1*^{null} homozygotes become fully penetrant in the *Hoxa1*^{null}/*Hoxb1*$^{3'RARE}$ double homozygotes, and abnormal exit of facial motor axons from r2 occurs only in the latter mutants. In *Hoxa1*^{null}/*Hoxb1*^{null} double homozygotes there are further defects in the development of cranial nerves, ganglia and motor neurons.

Early disruption of second pharyngeal arch development in *Hoxa1*^{null}/*Hoxb1*$^{3'RARE}$ double homozygotes

Hoxa1 and *Hoxb1* are not expressed in the second arch ectomesenchyme (Frohman et al., 1990; Murphy and Hill, 1991) and there are only minor defects in the mesenchymal neural crest derivatives of *Hoxa1*^{null} mutants (Lufkin et al., 1991; Mark et al., 1993) and no defects in those of *Hoxb1*^{null} homozygotes (Goddard et al., 1996; Studer et al., 1996). Strikingly, the combined lack of expression of *Hoxa1* and *Hoxb1* in the hindbrain synergistically results in aplasia of the second arch and ear defects reminiscent of certain human conditions that have their origin in defects of the first branchial arch and pouch (for a review, see Lambert and Dodson, 1996). The complete lack of second pharyngeal arch cartilage derivatives, the disruption of external and middle ear development, and the apparent lack of any ectopic cartilage elements in *Hoxa1*^{null}/*Hoxb1*$^{3'RARE}$ double homozygous 17.5 dpc fetuses and newborns (Table 2), are consistent with an early disruption of second pharyngeal arch development.

The second pharyngeal arch of the *Hoxa1*^{null} homozygotes appears to be hypoplastic at 10.5 dpc. This probably results from a reduction in the number of migrating neural crest cells caused either by the reduction in the size of the r4 territory, which provides the bulk of the second arch neural crest (Lumsden et al., 1991; Sechrist et al., 1993), and/or the rostral displacement of the otocyst, which may create a physical barrier (Mark et al., 1993). However, this reduction does not result in loss of second arch-derived elements, whereas the strong hypoplasia of the second arch in the *Hoxa1*^{null}/*Hoxb1*$^{3'RARE}$ double homozygotes has severe phenotypic consequences. Since NC cells are responsible for the patterning of the arch mesenchyme (Noden, 1983), a defect in this population may underlie the second arch involution phenotype. This is consistent with the early patterning defects in presumptive r4 territory of *Hoxa1*^{null}/*Hoxb1*$^{3'RARE}$ and *Hoxa1*^{null}/*Hoxb1*^{null} double homozygotes (Studer et al., 1998). Accordingly, expression of two NC markers, *CRABPI* (Mitchell et al., 1991) and *AP2* (Ruberte et al., 1992; Maden et al., 1992) is either abolished or further reduced in the second arch of double mutants at 9.25 dpc, as compared to *Hoxa1*^{null} homozygotes. *Hoxa1*^{null} homozygotes and double homozygotes are morphologically indistinguishable in the region of the pharyngeal arches at 9.25 dpc, but 1 day later only the second arch of the double homozygotes has involuted. This observation suggests a proliferative defect and/or excessive cell death of the second arch mesenchyme in the double homozygotes, although an early migratory problem of the second arch cells cannot be ruled out. Use of more NC markers and DiI labelling of migrating NC cells may allow us to distinguish between these possibilities.

A significant number of signalling molecules, such as *Fgf3* (Wilkinson et al., 1988; Mahmood et al., 1995), *Fgf4* (Niswander and Martin, 1992; Drucker and Goldfarb, 1993), *Fgf8* (Crossley and Martin, 1994; Heikinheimo et al., 1994) and *endothelin-1* (Kurihara et al., 1994) are expressed in the pharyngeal pouches, and the ectoderm of the pharyngeal arches. Their repetitive expression in the inter-arch regions suggests that they may be part of the signals that control growth and patterning of the pharyngeal arches. It is conceivable that the *Hox* code of the NC cells migrating from different axial levels (Hunt et al., 1991) enables them to perceive and interpret mitogenic and differentiation signals in order to generate the appropriate structures. The second pharyngeal arch NC cells of the double homozygotes may not be able to perceive these signals, ceasing, therefore, to proliferate, and resulting in the

observed aplasia of the second arch. Patterning of the pharyngeal endoderm may also be affected in the double homozygotes, thus compromising normal development of the second arch and contributing to the involution phenotype. However, the latter possibility is less likely, as *Hoxb1* expression is not abolished in the foregut of *Hoxa1*^{null}/*Hoxb1*$^{3'RARE}$ double homozygotes (Studer et al., 1998 and data not shown). It is also worth mentioning that *Hoxa3* null mutants show specific deletions or hypoplasias of structures derived or patterned by mesenchymal NC cells of the third pharyngeal arch (Chisaka and Capecchi, 1991; Manley and Capecchi, 1995). In these mutants, changes in overall generation or migration of NC cells are not observed, arguing for an intrinsic patterning (Manley and Capecchi, 1995) and/or proliferative defect once they have reached their destination.

The unexpected defects found in first arch-derived elements of *Hoxa1*^{null}/*Hoxb1*$^{3'RARE}$ double homozygotes are strikingly similar to those found in the *gsc* null mutants. *Gsc* null mutants lack the external auditory meatus, the tympanic ring, and exhibit hypoplasia of the manubrium and lack of the processus brevis of the malleus (Rivera-Pérez et al., 1995; Yamada et al., 1995). *Gsc* is expressed in the caudal mesenchyme of the first arch and the most rostral portion of the second, after completion of the NC cell migration (Gaunt et al., 1993). A hypothetical signalling center in this region was postulated to account for the phenotype of *Hoxa2* null mutants (Rijli et al., 1993), which have a set of duplicated first arch elements in place of second arch elements (Gendron-Maguire et al., 1993; Rijli et al., 1993). It is conceivable that the impaired second arch development, in the double mutants analysed here, affects this region as well, leading to first arch defects.

In summary, the early patterning defects in the presumptive r4 region of the double null homozygotes compromise correct specification of the second arch NC cells. This results in involution of the second arch and, consequently, complete disruption of external and middle ear development and loss of all second arch-derived elements. The defects observed in first arch-derived elements indicate that interactions between arches are part of the morphogenetic program in this region.

The authors would like to thank Jean-Luc Vonesch and Nadia Messaddeq for help with the electron and confocal microscopy, Robert Matyas for help with the dissection of the facial nerve and Betty Feret for excellent technical assistance. We are grateful to Manuel Mark and Georgy Köntges for discussions and comments on the manuscript. We thank G. Barsh for the *kr* probe, D. Wilkinson for the *Krox20*, P. Zelent for the *PLZF* and P. Mitchell for the *AP2* probe (Mitchell et al., 1991). The 2H3 monoclonal antibody was obtained from the Developmental Studies Hybridoma Bank maintained by The University of Iowa, Department of Biological Sciences, Iowa City, IA 52242, USA under contract NO1-HD-7-3263. A.G. was supported by fellowships from EC Human Capital Mobility, Fondation pour la Recherche Médicale (FRM) and a short term EMBO fellowship and M.S. was supported by fellowships from EMBO, EEC Human Capital Mobility and the Medical Research Council (MRC). This work was also supported by grants from the INSERM, CNRS, Collège de France, Association pour la Recherche sur le Cancer (ARC), FRM and LNC.

REFERENCES

Barrow, J. R. and Capecchi, M. R. (1996). Targeted disruption of the *Hob-2* locus in mice interferes with expression of *Hoxb*-1 and *Hoxb*-4. *Development* **122,** 3817-3828.

Carpenter, E. M., Goddard, J. M., Chisaka, O., Manley, N. R. and Capecchi, M. R. (1993). Loss of *Hox*-A1 (*Hox*-1.6) function results in the reorganization of the murine hindbrain. *Development* **118**, 1063-1075.

Chavrier, P., Zerial, M., Lemaire, P., Almendral, J., Bravo, R. and Charnay, P. (1988). A gene encoding a protein with zinc fingers is activated during G_0/G_1 transition in cultured cells. *EMBO J.* **7**, 29-35.

Chisaka, O. and Capecchi, M. R. (1991). Regionally restricted developmental defects resulting from targeted disruption of the mouse homeobox gene *Hox*-1.5 [see comments]. *Nature* **350**, 473-479.

Chisaka, O., Musci, T. S. and Capecchi, M. R. (1992). Developmental defects of the ear, cranial nerves and hindbrain resulting from targeted disruption of the mouse homeobox gene *Hox*-1.6 [see comments]. *Nature* **355**, 516-520.

Cooké, M., Gould, A., Brand, N., Davies, J., Strutt, P., Shaknovich, R., Licht, J., Waxman, S., Chen, Z., Gluecksohn-Waelsch, S., et al. (1995). Expression of the zinc-finger gene PLZF at rhombomere boundaries in the vertebrate hindbrain. *Proc. Nat. Acad. Sci. USA* **92**, 2249-2253.

Cordes, S. P. and Barsh, G. S. (1994). The mouse segmentation gene kr encodes a novel basic domain-leucine zipper transcription factor. *Cell* **79**, 1025-1034.

Couly, G. F., Coltey, P. M. and Le Douarin, N. M. (1993). The triple origin of skull in higher vertebrates: a study in quail-chick chimeras. *Development* **117**, 409-429.

Crossley, P. H. and Martin, G. R. (1995). The mouse Fgf8 gene encodes a family of polypeptides and is expressed in regions that direct outgrowth and patterning in the developing embryo. *Development* **121**, 439-451.

D'Amico-Martel, A. and Noden, D. M. (1983). Contributions of placodal and neural crest cells to avian cranial peripheral ganglia. *Am. J. Anat.* **166**, 445-468.

Dollé, P., Lufkin, T., Krumlauf, R., Mark, M., Duboule, D. and Chambon, P. (1993). Local alterations of Krox-20 and *Hox* gene expression in the hindbrain suggest lack of rhombomeres 4 and 5 in homozygote null *Hox*a-1 (*Hox*-1. 6) mutant embryos. *Proc. Nat. Acad. Sci. USA* **90**, 7666-7670.

Drucker, B. J. and Goldfarb, M. (1993). Murine FGF-4 gene expression is spatially restricted within embryonic skeletal muscle and other tissues. *Mech. Dev.* **40**, 155-163.

Dupé, V., Davenne, M., Brocard, J., Dollé, P., Mark, M., Dierich, A., Chambon, P. and Rijli, F. M. (1997). In vivo functional analysis of the *Hox*a-1 3′ retinoic acid response element (3′RARE). *Development* **124**, 399-410.

Favier, B. and Dollé, P. (1997). Developmental functions of mammalian *Hox* genes. *Mol. Hum. Reprod.* **3**, 115-131.

Fraser, S., Keynes, R. and Lumsden, A. (1990). Segmentation in the chick embryo hindbrain is defined by cell lineage restrictions. *Nature* **344**, 431-435.

Frohman, M. A., Boyle, M. and Martin, G. R. (1990). Isolation of the mouse *Hox*-2. 9 gene; analysis of embryonic expression suggests that positional information along the anterior-posterior axis is specified by mesoderm. *Development* **110**, 589-607.

Frohman, M. A., Martin, G. R., Cordes, S. P., Halamek, L. P. and Barsh, G. S. (1993). Altered rhombomere-specific gene expression and hyoid bone differentiation in the mouse segmentation mutant, kreisler (kr). *Development* **117**, 925-936.

Gale, E., Prince, V., Lumsden, A., Clarke, J., Holder, N. and Maden, M. (1996). Late effects of retinoic acid on neural crest and aspects of rhombomere. *Development* **122**, 783-793.

Gaunt, S. J., Blum, M. and De Robertis, E. M. (1993). Expression of the mouse goosecoid gene during mid-embryogenesis may mark mesenchymal cell lineages in the developing head, limbs and body wall. *Development* **117**, 769-778.

Gavalas, A., Davenne, M., Lumsden, A., Chambon, P. and Rijli, F. M. (1997). Control of axon guidance and rostral hindbrain patterning by *Hoxa-2*. *Development* **124**, 3693-3702.

Gendron-Maguire, M., Mallo, M., Zhang, M. and Gridley, T. (1993). *Hox*a-2 mutant mice exhibit homeotic transformation of skeletal elements derived from cranial neural crest. *Cell* **75**, 1317-1331.

Goddard, J. M., Rossel, M., Manley, N. R. and Capecchi, M. R. (1996). Mice with targeted disruption of *Hox*b-1 fail to form the motor nucleus of the VIIth nerve. *Development* **122**, 3217-3228.

Graham, A., Francis-West, P., Brickell, P. and Lumsden, A. (1994). The signalling molecule BMP4 mediates apoptosis in the rhombencephalic neural crest. *Nature* **372**, 684-686.

Graham, A., Heyman, I. and Lumsden, A. (1993). Even-numbered rhombomeres control the apoptotic elimination of neural crest cells from odd-numbered rhombomeres in the chick hindbrain. *Development* **119**, 233-245.

Guthrie, S. and Lumsden, A. (1991). Formation and regeneration of rhombomere boundaries in the developing chick hindbrain. *Development* **112**, 221-229.

Guthrie, S., Prince, V. and Lumsden, A. (1993). Selective dispersal of avian rhombomere cells in orthotopic and heterotopic grafts. *Development* **118**, 527-538.

Heikinheimo, M., Lawshe, A., Shackleford, G. M., Wilson, D. B. and MacArthur, C. A. (1994). Fgf-8 expression in the post-gastrulation mouse suggests roles in the development of the face, limbs and central nervous system. *Mech. Dev.* **48**, 129-138.

Hunt, P., Guilisano, M., Cook, M., Sham, M.-H., Faiella, A., Wilkinson, D., Boncinelli, E. and Krumlauf, R. (1991). A distinct Hox code for the branchial region of the vertebrate head. *Nature* **353**, 861-864.

Kessel, M. (1993). Reversal of axonal pathways from rhombomere 3 correlates with extra *Hox* expression domains. *Neuron* **10**, 379-393.

Keynes, R. and Krumlauf, R. (1994). *Hox* genes and regionalization of the nervous system. *Annu. Rev. Neurosci.* **17**, 109-132.

Keynes, R. and Lumsden, A. (1990). Segmentation and the origin of regional diversity in the vertebrate central nervous system. *Neuron* **4**, 1-9.

Köntges, G. and Lumsden, A. (1996). Rhombencephalic neural crest segmentation is preserved throughout craniofacial ontogeny. *Development* **122**, 3229-3242.

Kurihara, Y., Kurihara, H., Suzuki, H., Kodama, T., Maemura, K., Nagai, R., Oda, H., Kuwaki, T., Cao, W. H., Kamada, N., et al. (1994). Elevated blood pressure and craniofacial abnormalities in mice deficient in endothelin-1 [see comments]. *Nature* **368**, 703-710.

La Rosa, G. J. and Gudas, L. J. (1988). Early retinoic acid-induced F9 teratocarcinoma stem cell gene ERA-1: alternate splicing creates transcripts for a homeobox-containing protein and one lacking the homeobox. *Mol. Cell Biol.* **8**, 3906-3917.

Lambert, P. R. and Dodson, E. E. (1996). Congenital malformations of the external auditory canal. *Otolaryngol. Clin. North Am.* **29**, 741-760.

Le Lievre, C. S. and Le Douarin, N. M. (1975). Mesenchymal derivatives of the neural crest: analysis of chimaeric quail and chick embryos. *J. Embryol. exp. Morph.* **34**, 125-154.

Lufkin, T., Dierich, A., Le Meur, M., Mark, M. and Chambon, P. (1991). Disruption of the *Hox*-1. 6 homeobox gene results in defects in a region corresponding to its rostral domain of expression. *Cell* **66**, 1105-110|.

Lumsden, A. and Keynes, R. (1989). Segmental patterns of neuronal development in the chick hindbrain. *Nature* **337**, 424-428.

Lumsden, A. and Krumlauf, R. (1996). Patterning the vertebrate neuraxis. *Science* **274**, 1109-1115.

Lumsden, A., Sprawson, N. and Graham, A. (1991). Segmental origin and migration of neural crest cells in the hindbrain region of the chick embryo. *Development* **113**, 1281-1291.

Maconochie, M., Nonchev, S., Studer, M., Chan, S.-K., Pöpperl, H., Sham, M.-H., Mann, R. and Krumlauf, R. (1997). Cross-regulation in the mouse HoxB complex: the expression of Hoxb2 in rhombomere 4 is regulated by Hoxb1. *Genes Dev.* **11**, 1885-1896.

Maden, M., Horton, C., Graham, A., Leonard, L., Pizzey, J., Siegenthaler, G., Lumsden, A. and Eriksson, U. (1992). Domains of cellular retinoic acid-binding protein I (CRABP I) expression in the hindbrain and neural crest of the mouse embryo. *Mech. Dev.* **37**, 13-23.

Mahmood, R., Kiefer, P., Guthrie, S., Dickson, C. and Mason, I. (1995). Multiple roles for FGF-3 during cranial neural development in the chicken. *Development* **121**, 1399-1410.

Manley, N. R. and Capecchi, M. R. (1995). The role of *Hox*a-3 in mouse thymus and thyroid Development *Development* **121**, 1989-2003.

Manzanares, M., Cordes, S., Kwan, C.-T., Sham, M. H., Barsh, G. S. and Krumlauf, R. (1997). Segmental regulation of *Hox*b-3 by kreisler. *Nature* **387**, 191-195.

Mark, M., Lohnes, D., Mendelsohn, C., Dupé V., Vonesch, J. L., Kastner, P., Rijli, F. M., Bloch-Zupan, A. and Chambon, P. (1995). Roles of retinoic acid receptors and of *Hox* genes in the patterning of the teeth and of the jaw skeleton. *Int. J. Dev. Biol.* **39**, 111-121.

Mark, M., Lufkin, T., Vonesch, J. L., Ruberte, E., Olivo, J. C., Dolle, P., Gorry, P., Lumsden, A. and Chambon, P. (1993). Two rhombomeres are altered in *Hox*a-1 mutant mice. *Development* **119**, 319-338.

Marshall, H., Nonchev, S., Sham, M. H., Muchamore, I., Lumsden, A. and Krumlauf, R. (1992). Retinoic acid alters hindbrain *Hox* code and induces transformation of rhombomeres 2/3 into a 4/5 identity [see comments]. *Nature* **360**, 737-741.

McKay, I. J., Muchamore, I., Krumlauf, R., Maden, M., Lumsden, A. and Lewis, J. (1994). The kreisler mouse: a hindbrain segmentation mutant that lacks two rhombomeres. *Development* **120**, 2199-2211.

Mitchell, P. J., Timmons, P. M., Hebert, J. M., Rigby, P. W. and Tjian, R. (1991). Transcription factor AP-2 is expressed in neural crest cell lineages during mouse embryogenesis. *Genes Dev.* **5**, 105-10|.

Moody, S. A. and Heaton, M. B. (1983). Developmental relationships between trigeminal ganglia and trigeminal motoneurons in chick embryos. I. Ganglion development is necessary for motoneuron migration. *J. Comp. Neurol.* **213**, 327-343.

Murphy, P. and Hill, R. E. (1991). Expression of the mouse labial-like homeobox-containing genes, *Hox* 2. 9 and *Hox* 1. 6, during segmentation of the hindbrain. *Development* **111**, 61-74.

Niederlander, C. and Lumsden, A. (1996). Late emigrating neural crest cells migrate specifically to the exit points of cranial branchiomotor nerves. *Development* **122**, 2367-2374.

Niswander, L. and Martin, G. R. (1992). Fgf-4 expression during gastrulation, myogenesis, limb and tooth development in the mouse. *Development* **114**, 755-768.

Nittenberg, R., Patel, K., Joshi, Y., Krumlauf, R., Wilkinson, D. G., Brickell, P. M., Tickle, C. and Clarke, J. D. (1997). Cell movements, neuronal organisation and gene expression in hindbrains lacking morphological boundaries. *Development* **124**, 2297-2306.

Noden, D. M. (1988). Interactions and fates of avian craniofacial mesenchyme. *Development* **103 Supplement**, 121-140.

Noden, D. M. (1983). The role of the neural crest in patterning of avian cranial skeletal, connective, and muscle tissues. *Dev. Biol.* **96**, 144-165.

Noden, D. M. and Van de Water, T. R. (1992). The developing ear: tissue origins and interactions. In *The Biology of Changes in Otolaryngology* (ed. R. W. Ruben, T. R. Van de Water and E. W. Rubel), pp. 15-46. New York: Elsevier.

Nonchev, S., Vesque, C., Maconochie, M., Seitanidou, T., Ariza-McNaughton, L., Frain, M., Marshall, H., Sham, M. H., Krumlauf, R. and Charnay, P. (1996). Segmental expression of *Hox*a-2 in the hindbrain is directly regulated by Krox-20. *Development* **122**, 543-554.

Pöpperl, H., Bienz, M., Studer, M., Chan, S.-K., Aparicio, S., Brenner, S., Mann, R. S. and Krumlauf, R. (1995). Segmental expression of *Hoxb-1* is controlled by a highly conserved autoregulatory loop dependent on *exd/pbx*. *Cell* **81,** 1031-1042.

Rijli, F. M., Mark, M., Lakkaraju, S., Dierich, A., Dollé, P. and Chambon, P. (1993). A homeotic transformation is generated in the rostral branchial region of the head by disruption of *Hox*a-2, which acts as a selector gene. *Cell* **75**, 1333-1349.

Rijli, F. M. and Chambon, P. (1997). Genetic interactions of *Hox* genes in limb development: learning from compound mutants. *Curr. Opin. Genet. Dev. Biol.* **7**, 481-487.

Rivera-Perez, J. A., Mallo, M., Gendron-Maguire, M., Gridley, T. and Behringer, R. R. (1995). Goosecoid is not an essential component of the mouse gastrula organizer but is required for craniofacial and rib development. *Development* **121**, 3005-3012.

Ruberte, E., Friederich, V., Morriss-Kay, G. and Chambon, P. (1992). Differential distribution patterns of CRABP I and CRABP II transcripts during mouse embryogenesis. *Development* **115**, 973-987.

Schneider-Maunoury, S., Seitanidou, T., Charnay, P. and Lumsden, A. (1997). Segmental and neuronal architecture of the hindbrain of Krox-20 mouse mutants. *Development* **124**, 1215-1226.

Schneider-Maunoury, S., Topilko, P., Seitandou, T., Levi, G., Cohen-Tannoudji, M., Pournin, S., Babinet, C. and Charnay, P. (1993). Disruption of Krox-20 results in alteration of rhombomeres 3 and 5 in the developing hindbrain. *Cell* **75**, 119-214.

Schörle, H., Meier, P., Buchert, M., Jaenisch, R. and Mitchell, P. J. (1996). Transcription factor AP-2 essential for cranial closure and craniofacial development. *Nature* **381**, 235-238.

Sechrist, J., Serbedzija, G. N., Scherson, T., Fraser, S. E. and Bronner-Fraser, M. (1993). Segmental migration of the hindbrain neural crest does not arise from its segmental generation. *Development* **118**, 691-703.

Seitanidou, T., Schneider-Maunoury S., Desmarquet C., Wilkinson, D. G. and Charnay, P. (1997). Krox-20 is a key regulator of rhombomere-specific gene expression in the developing hindbrain. *Mech. Dev*. **65**, 31-42.

Sham, M. H., Vesque, C., Nonchev, S., Marshall, H., Frain, M., Gupta, R. D., Whiting, J., Wilkinson, D., Charnay, P. and Krumlauf, R. (1993). The zinc finger gene Krox20 regulates *Hox*B2 (*Hox*2. 8) during hindbrain segmentation. *Cell* **72**, 183-196.

Studer, M., Lumsden, A., Ariza-McNaughton, L., Bradley, A. and Krumlauf, R. (1996). Altered segmental identity and abnormal migration of motor neurons in mice lacking *Hox*b-1. *Nature* **384**, 630-634.

Studer, M., Gavalas A., Marshall, H., Ariza-McNaughton, L., Rijli, F. M., Chambon, P. and Krumlauf, R. (1998). Genetic interactions between *Hoxa1* and *Hoxb1* reveal additional roles in regulation of early hindbrain patterning. *Development* **125,** 1025-1036.

Swiatek, P. J. and Gridley, T. (1993). Perinatal lethality and defects in hindbrain development in mice homozygous for a targeted mutation of the zinc finger gene Krox20. *Genes Dev.* **7**, 2071-2084.

Taneja, R., Thisse, B., Rijli, F. M., Thisse, C., Bouillet, P., Dolle, P. and Chambon, P. (1996). The expression pattern of the mouse receptor tyrosine kinase gene MDK1 is conserved through evolution and requires *Hox*a-2 for rhombomere-specific expression in mouse embryos. *Dev. Biol.* **177**, 397-412.

Trainor, P. A. and Tam, P. P. (1995). Cranial paraxial mesoderm and neural crest cells of the mouse embryo: co-distribution in the craniofacial mesenchyme but distinct segregation in branchial arches. *Development* **121**, 2569-2582.

Vesque, C., Maconochie, M., Nonchev, S., Ariza-McNaughton, L., Kuroiwa, A., Charnay, P. and Krumlauf, R. (1996). *Hox*b-2 transcriptional activation in rhombomeres 3 and 5 requires an evolutionarily conserved cis-acting element in addition to the Krox-20 binding site. *EMBO J.* **15**, 5383-5396.

Wilkinson, D. G. (1995). Genetic control of segmentation in the vertebrate hindbrain. *Perspect. Dev. Neurobiol.* **3**, 29-38.

Wilkinson, D. G., Bhatt, S., Chavrier, P., Bravo, R. and Charnay, P. (1989a). Segment-specific expression of a zinc-finger gene in the developing nervous system of the mouse. *Nature* **337**, 461-464.

Wilkinson, D. G., Bhatt, S., Cook, M., Boncinelli, E. and Krumlauf, R. (1989b). Segmental expression of *Hox*-2 homoeobox-containing genes in the developing mouse hindbrain. *Nature* **341**, 405-409.

Wilkinson, D. G., Peters, G., Dickson, C. and McMahon, A. P. (1988). Expression of the FGF-related proto-oncogene int-2 during gastrulation and neurulation in the mouse. *EMBO J.* **7**, 691-695.

Wingate, R. J. and Lumsden, A. (1996). Persistence of rhombomeric organisation in the postsegmental hindbrain. *Development* **122**, 2143-2152.

Yamada, G., Mansouri, A., Torres, M., Stuart, E. T., Blum, M., Schultz, M., De Robertis, E. M. and Gruss, P. (1995). Targeted mutation of the murine goosecoid gene results in craniofacial defects and neonatal death. *Development* **121**, 2917-2922.

Zhang, J., Hagopian-Donaldson, S., Serbedzija, G., Elsemore, J., Plehn-Dujowich, D., McMahon, A. P., Flavell, R. A. and Williams, T. (1996). Neural tube, skeletal and body wall defects in mice lacking transcription factor AP-2. *Nature* **381**, 238-241.